THREE COLOUR PHOTOMETRY OF GALACTIC CLUSTERS

NGC 2422, NGC 2423 and NGC 2437

A Thesis submitted to the
University of Edinburgh
for the degree of

MASTER OF SCIENCE

by

KASHI NATH NANDY, B.Sc. (Cal.) M.Sc. (Cal.)

OCTOBER, 1961.

ABSTRACT

The work is described in two parts.

Part I contains a discussion of the work on the interpretation of the Hertzsprung-Russell diagram with regard to problems of stellar evolution .

Part II describes the three-colour studies of the southern galactic clusters NGC 2422, NGC 2423, and NGC 2437. The colour excesses and distances, corrected for absorption, are: NGC 2422, $0.^{m}06$ and 480 parsecs; NGC 2423, 0 and 450 parsecs; NGC 2437, $0.^{m}16$, 1450 parsecs.

C O N T E N T S

INTRODUCTION

For the last ten years the galactic star clusters have provided valuable information regarding (a) the evolution of stars, and (b) the structure and development of our galaxy. In this essay I have attempted to outline the present status of the problems concerning the interpretation of the H-R diagrams of clusters in terms of modern evolutionary theories. The discussion has been illustrated by the detailed investigation of three southern galactic clusters the plates of which had been taken by a number of observers at the Boyden Observatory in South Africa.

The study of star clusters is relevant in our approach to the construction of a theory of stellar evolution because star clusters furnish a group of stars which, it is commonly held, were formed from the same galactic material at closely the same time. The composition of galactic material may have shown differences in separate large regions, but it may be assumed that the composition is uniform in comparatively small regions. It appears thus reasonable to assume that the material out of which a cluster has formed had uniform composition. The basic theory of stellar structure states that the position of a star in the H-R diagram depends on its mass, its initial composition, and its age. Therefore the H-R diagrams of star clusters represent the instantaneous locus of stages through which stars of different masses, but

of similar composition and of the same age, are passing. Differences in the diagrams can be interpreted in terms of differences in age and initial composition. From theory, the distribution of stars in H-R diagrams can be predicted, and theories can thus be compared with observation.

It is possible to discriminate between open and globular clusters on the basis of their distribution in the galaxy. Open or galactic clusters, groups of from dozens to hundreds of stars, are found exclusively in the principal plane of the Milky Way and are distributed irregularly throughout all galactic longitudes. They are often embedded in dust clouds, as in the case of NGC 2264. Globular clusters which are groups of 10^5 stars approximately are, on the other hand, scattered in galactic latitude.

The systematic study of galactic clusters was initiated by Trumpler in 1920. Using apparent magnitude and spectral type he derived for each cluster a diagram analogous to the well-known H-R diagrams for field stars. Trumpler's diagrams showed the existence of a variety of types of galactic clusters. Clusters which do not contain O and B type stars, such as the Hyades, contain an appreciable number of red giants. In some clusters, such as the Pleiades, the main-sequence is well represented but red giants are absent. Trumpler classified the galactic clusters, according to the form and position of their sequences, into 1b, 1a and 2a through 2f types; he also correlated linear diameter with the cluster

type.

In 1930, from the study of the relation between diameters and distances of clusters, Trumpler was the first to produce evidence of interstellar absorption and to derive an average value for the coefficient of absorption by interstellar material - 0.7 mag. per kiloparsec.

Shapley's almost simultaneous studies of globular and galactic clusters revealed striking differences in their colour-magnitude diagrams, though his observations did not extend to stars with absolute magnitudes fainter than +1. While the diagrams of galactic clusters showed a variety of forms, globular clusters appeared to be distinguished by one and the same diagram. As Shapley pointed out already at that time, "Time seems to leave its mark on the clusters along the Milky Way." Among other early contributors to the progress of the study of open clusters, Collinder published an extensive bibliography of open clusters known up to 1931.

The results of early observations on open clusters can perhaps be summarised thus:- The H-R diagrams of individual clusters show less scatter in their main sequences than the H-R diagram for stars in general. However, when the main sequences of several clusters are fitted together, systematic deviations occurred between the positions of luminous main sequence stars. To explain these diagrams Kuiper postulated in 1937 a hypothesis on the basis of work by B. Strömgren, who had concluded that mass and hydrogen content determine a star's

position in the H-R diagram. Kuiper postulated that galactic clusters are groups of stars which have the same hydrogen content.

The modern observational work began with H. Haffner and O. Heckmann's accurate photometric studies of Praesepe. It was found that the stars of this cluster redder than $B - V = 0.3^m$ define a very narrow main sequence. Haffner's work was followed by photoelectric observations of Eggen, Johnson and others on Hyades, Praesepe, Pleiades and other open clusters. Accuracy achieved by the photoelectric method has required a revision of the problem of the zero-point in stellar photometry.

Also, it was discovered that the measures of colours in early observations, especially on the A stars which are plentiful in open clusters, were somewhat distorted by the effect of hydrogen absorption near the Balmer limit. This may cause differences between magnitudes on various photometric systems. Moreover, observed colours have to be corrected for the effect of interstellar reddening.

Multicolour photometry, initiated by W. Becker and subsequently developed by Johnson and Morgan, has provided a means of determining interstellar reddening and absorption without knowing spectral types. The difficulty with hydrogen absorption at shorter wavelengths has been taken care of by Johnson and Morgan in their U, B, V system which, for the present at least, can be regarded as the standard photometric

system. The rapid advance in the study of the H-R diagrams of clusters is largely due to the introduction of this system.

Recent photometric observations for field stars with known trigonometric parallaxes and for clusters whose distances are well determined such as the Hyades show that the main sequences of field stars and clusters form a narrow band below $M_V = +5$. Combining these photometric observations with a theory of stellar evolution Johnson and others have derived a "standard main sequence" with which part of the colour-magnitude diagram of any cluster will be identical. Thus star clusters may play an important role as secondary distance indicators.

Indications of age come from a number of sources:-

(1) Dynamical studies of the galactic system suggest that most galactic clusters cannot exceed the age of about 5×10^9 years, being unable to withstand tidal distortions from the gravitational sources, whereas globular clusters are more stable and may remain undistorted for many billion years.

(2) Considering the masses of supergiants and their rate of radiation it is evident that supergiants can have been formed only recently. Modern theories of nuclear energy generation point to a differential rate of evolution - the luminous and more massive stars must evolve more quickly than the less luminous stars of small mass.

(3) There exists a significant correlation between the

physical characteristics and the kinematic behaviour of stars in the solar neighbourhood. Some of the late type stars are characterised by high space velocities, which is due to their having entered the Sun's vicinity from other parts of the galaxy. The smallest space-velocities are found for O and B stars; and their average space velocity is nearly the same as that of the interstellar gas and dust. The high velocities of some stars presumably reflect a high initial turbulence of matter in the early stages of the galaxy; high velocity stars are likely to be old. As expected, the colour-magnitude diagram of these high velocity stars resembles, in its main features, those of globular clusters. The low velocity stars, on the other hand, when plotted in a colour-magnitude diagram, lie in an array similar to those of galactic clusters.

Fitting observed cluster-sequences to the standard main sequence Sandage has derived a procedure for dating clusters.

In 1944 Baade suggested that galactic clusters and globular clusters belong to different "stellar populations". Through his work on the centre of the Andromeda Nebula and its two elliptical companions, he was led to believe the existence of two types of population, population I and population II, among the stars of our galaxy. Typical examples of population I are O and B stars, galactic clusters, classical cepheids and the stellar associations,

which are all spiral arm objects. Typical examples of population II are the globular clusters in the halo of our galaxy.

Baade's suggestion has brought marked advances in several directions, one of them being the location of spiral arms by members of population I. Knowledge of accurate distances and ages of open clusters promises to give data on the problem of galactic structure and evolution.

PART I

CHAPTER I

METHODS OF DETERMINING THE DISTRIBUTION OF STARS IN THE H-R DIAGRAM

Photometric Systems

In order to make the H-R diagram interpretable in terms of astrophysical theories, the observed parameters have to be related to luminosity and effective temperature. Luminosity is measured in bolometric magnitudes which give the total energy over the whole stellar spectrum. The relation between luminosity and bolometric magnitude is given by

$$M_{Bol} = -2.5 \log L + K \quad , \qquad (1.1)$$

where K is a constant defining the zero point of the scale.

The quantities obtained by photometric observations are apparent magnitudes which measure the light intensity effective on the receiver over limited wavelength regions. The colour index is the difference between the magnitudes in two relatively short wavelength regions. It can be calibrated in terms of colour temperature, a parameter in Planck's formula which expresses the intensity distribution in part of the spectrum of the star.

If the distance of the star is known, the absolute magnitude of the star for the wavelength region in question is given by

$$M = m + 5 - 5 \log D \quad , \qquad (1.2)$$

where M, m are the absolute and apparent magnitudes respectively and D is the distance in parsec.

The reduction of absolute magnitude to bolometric magnitude is achieved by applying a bolometric correction. This depends on surface temperature and so is known as a function of colour index.

Effective temperature is the temperature of the black body of equal radius which emits the same amount of energy as the star, and it is defined by the relation

$$L = 4\pi R^2 \sigma T_e^4 \qquad (1.3)$$

where R and T_e are the radius and effective temperature of the star.

This physical parameter is not readily obtainable for most stars, as stars do not radiate like black bodies. However, the six-colour photometry of Stebbins and Whitford (1945) has shown that the star's observed spectral distribution over a certain range can be represented by Planck's formula at some temperature, which is called the colour temperature. Using colour-temperatures to interpolate between stars of different effective temperatures which have been determined accurately, a scale between intrinsic colour indices and effective temperatures can be set up.

Thus from the observed quantities, an absolute magnitude - colour index diagram can be converted into a luminosity -

effective temperature diagram; the conversions of observed quantities to theoretical quantities are still carried through semi-empirically.

For an intercomparison of results obtained by different workers, these quantities have to be reduced to a standard system. Standard photometric systems are defined by specifying colour filters and light receivers. The zero-point of the magnitude scale in the standard system is well defined by a standard magnitude sequence.

However, a given system cannot be reproduced with absolute precision. It is often necessary to reduce an observational system to the standard system. This requires that magnitude in different systems should be linearly related. Assuming that stars radiate like black bodies the absolute magnitude at wavelength λ, M_λ is given by

$$M_\lambda = C_\lambda - 5 \log R + \frac{1.561}{\lambda . T} + 2.5 \log \left(1 - e^{-c_2/\lambda T}\right) \qquad (1.4)$$

where C_λ is a constant depending on wavelength.
If $\frac{c_2}{\lambda . T}$ is fairly large, the contribution from the last term is negligible.

The colour index, which is the difference in the magnitudes at two wavelengths λ_A and λ_B, say, is given by

$$I_c = M_{\lambda_A} - M_{\lambda_B}$$
$$= \left(C_{\lambda_A} - C_{\lambda_B}\right) + \frac{1.561}{T} \cdot \left(\frac{1}{\lambda_A} - \frac{1}{\lambda_B}\right) \qquad (1.5)$$

Let the magnitudes be measured at λ_A, and λ_B, with the condition that (λT) is small. Then the relation between I_C' in the new system and I_C is

$$I_C = \alpha . I_C' + \beta \tag{1.6}$$

where $\alpha = \dfrac{\frac{1}{\lambda_A} - \frac{1}{\lambda_B}}{\frac{1}{\lambda_{A'}} - \frac{1}{\lambda_{B'}}}$

and $\beta = (C_{\lambda_A} - C_{\lambda_B}) - \alpha . (C_{\lambda_{A'}} - C_{\lambda_{B'}})$

The magnitude $M_{\lambda_{A'}}$ is related to M_{λ_A} by the equation

$$M_{\lambda_A} = M_{\lambda_{A'}} + \gamma . I_C' + \delta \tag{1.7}$$

where $\gamma = \dfrac{\frac{1}{\lambda_A} - \frac{1}{\lambda_{A'}}}{\frac{1}{\lambda_{A'}} - \frac{1}{\lambda_{B'}}}$

and $\delta = (C_{\lambda_A} - C_{\lambda_{A'}}) - \gamma . (C_{\lambda_{A'}} - C_{\lambda_{B'}})$

α, β, γ and δ are constant for all T.

The linearity of relations (1.6) and (1.7) between different sets of monochromatic magnitudes depends however on the conditions specified.

In practice, magnitudes are measured over a range of wavelength depending on the sensitivity of the receiver and the transmission of the filter employed. The question arises whether a heterochromatic magnitude represents a monochromatic magnitude at some wavelength λ, called the equivalent wavelength, within the band. Let $\phi(\lambda)$ be the sensitivity of the

receiver with filter, optical train and atmosphere. Then the total flux effective on the receiver is given by

$$I = \int_0^\infty I(\lambda)\, \phi(\lambda)\, d\lambda \tag{1.8}$$

where $I(\lambda)$ = energy emitted by the star per second at wavelength λ per unit cross-section incident normally on the top of the atmosphere.

Assuming $I(\lambda)$ is continuous in the neighbourhood of λ_0, $I(\lambda)$ can be expanded in a Taylor's series,

$$I = I(\lambda_0) \int_0^\infty \phi(\lambda)\, d\lambda + I'(\lambda_0) \int_0^\infty (\lambda - \lambda_0)\, \phi(\lambda)\, d\lambda + \tfrac{1}{2} I''(\lambda_0) \int_0^\infty (\lambda - \lambda_0)^2 \phi(\lambda)\, d\lambda + \cdots\cdots \tag{1.9}$$

Wesselink (1950) made the approximation that second and higher derivatives of $I(\lambda)$ can be ignored. Then

$$I = I(\lambda_0) \int_0^\infty \phi(\lambda)\, d\lambda \tag{1.10}$$

where λ_0 is given by

$$\int_0^\infty (\lambda - \lambda_0)\, \phi(\lambda)\, d\lambda = 0$$

$$\text{i.e.} \quad \lambda_0 = \frac{\int_0^\infty \lambda\, \phi(\lambda)\, d\lambda}{\int_0^\infty \phi(\lambda)\, d\lambda} \tag{1.11}$$

Thus the magnitude of a star measured over a wavelength range can be represented by a monochromatic magnitude at the equivalent

wavelength λ_o, with a possible change of zero-point, and the equations (1.4) - (1.7) can be used, provided the star does not show any abrupt variation of energy distribution within the band. These relations have greatly simplified reductions to a standard system of magnitude.

Greaves (1952) has pointed out that the effect of spectral lines within the band will limit the accuracy obtained by reduction processes to 0.01 magnitude.

The International System has been widely used in the past as Standard System, the Mount Wilson North Polar Sequence observed by F.H. Sears providing both photographic and photo-visual magnitudes. For high precision the International System is inadequate for the following reasons:-

(a) the inadequacy of the North Polar Sequence for the definition of the standard zero-point. A standard system should include magnitudes and colour indices for unreddened stars in all regions of the H-R diagram and the same data for reddened stars of all known spectral types. The North Polar Sequence does not contain many types of stars. With the limited number of types of stars, a transformation of sufficient accuracy is not possible. Furthermore, it is now known that the North Pole region is not free from interstellar reddening. A two colour system is not adequate to distinguish between reddened blue stars and intrinsically red stars.

In many cases photometric values on the International system obtained by different observers were not in good agreement. Stoy (1956) has drawn attention to a considerable

disagreement on the exact definition of the International System for NPS stars. Stebbins and Whitford (1938) have found a scale error in the magnitude of some bright North Polar Sequence stars. These were confirmed by Eggen (1950), and other observers.

(b) inclusion of ultraviolet radiation. An unknown amount of ultraviolet radiation is included in the International photographic magnitude. Johnson (1952a) has shown that if radiation of wavelength shorter than 3800A is included in the measurements, the transformation from one system to another becomes non-linear and sometimes multi-valued. This difficulty arises due to the presence of strong Balmer lines in the spectra of hotter stars.

Multicolour Photometry

In the spectra of early-type stars the intensity of the continuous spectrum shows a marked discontinuity at the limit of the Balmer series at 3646A. The amount of the Balmer discontinuity depends on temperature, and on the extent to which hydrogen contributes to the total opacity. A graph of the Balmer discontinuity against spectral type shows that it rises from B0 to a maximum at A0 and then decreases as temperature decreases. For stars earlier than A0, hydrogen is strongly ionized. The Balmer discontinuity which now measures the ratio of the Balmer continuous

absorption to that of Paschen and higher continua, steadily decreases with increasing temperature. Later than A0, the contribution of neutral hydrogen to the total opacity decreases as compared with that of the negative hydrogen ion.

It thus appears that the Balmer absorption gives important clues to the physical nature of the stars and that its effect can be used in the study of the luminosity problem. At least one other colour-index is required, however.

The first attempt to provide this was made by W. Becker (1948) who showed, by using a third equivalent wavelength in the ultraviolet, how intrinsic reddening can be separated from external space reddening. The six-colour photometry of Stebbins and Whitford was another step in the pursuit of multicolour photometry. One of the important results of their work is the determination of the law of interstellar reddening.

In 1952 Becker suggested the selection of spectral regions at equivalent wavelengths 6400A, 4700A and 3700A (I.A.U. Trans. 8, 355, 1952). In the 3700A region the deviation from black body radiation appears in the form of Balmer absorption. The intensity distribution between 6400A and 4700A is suitable for determining colour temperature.

U, B, V System

In 1953 Johnson and Morgan (1953) outlined a standard

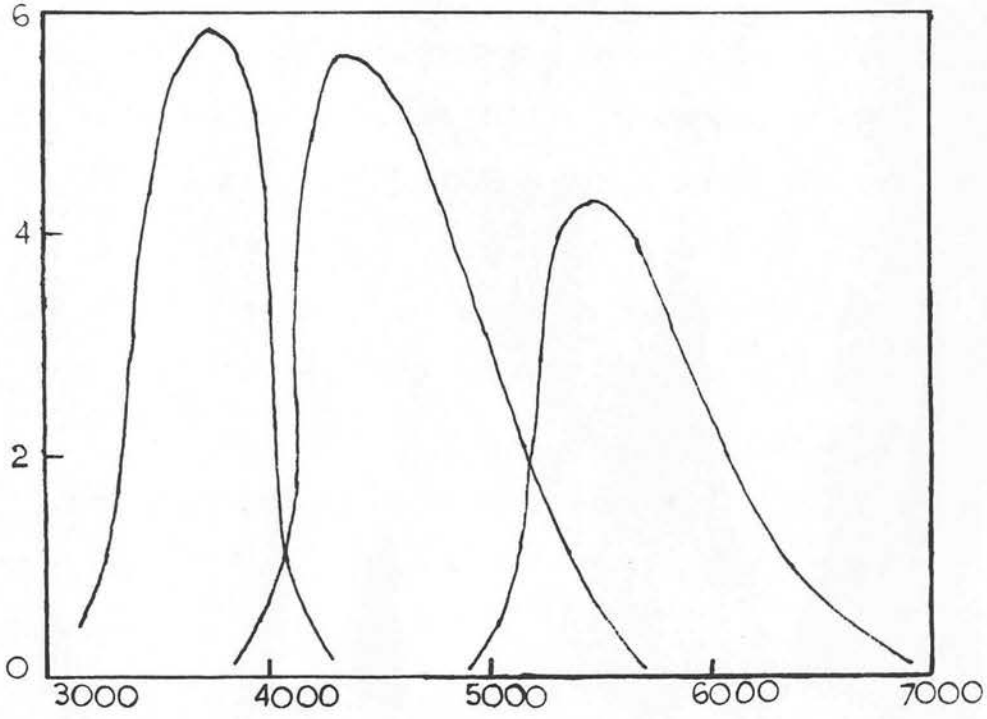

FIG. 1— Spectral response against wavelength.
From Johnson (1955).

three-colour photometric system for the purposes of photoelectric and photographic photometry. They have excluded light of wavelength shorter than 3800A from the B magnitude by using a suitable filter and have defined an ultraviolet colour-index U-B. The effects of the Balmer absorption are confined to the U-magnitudes secured by means of a 2 mm Schott UG2 filter. The V magnitude corresponds to the former International photovisual magnitude. The zero-point for all colour systems has been set up by using the mean values for six stars of class A0V on the MK system. For these means,

$$U - B = B - V = 0 \qquad (1.12)$$

where U = observed magnitude through the ultraviolet filter,
B = observed magnitude through the blue filter,
and V = observed magnitude through the yellow filter,
all magnitudes reduced to outside the Earth's atmosphere. The U, B, V system is based on the observations made with a filter-photomultiplier combination which has spectral responses in the three wavelength bands as shown in Figure 1. (Johnson, 1955).

The response in the U band extends from about λ3000 to 4000A with equivalent wavelength about 3600A, in the B band from about λ3900 to 5500A, with equivalent wavelength about 4300A, and in the V band from about λ4900 to 6500A with equivalent wavelength about 5500A.

The filters recommended for defining the U, B, V system are the following (I.A.U. Symposium No. 7, p. 91, 1959):-

(a) For photoelectric observation

U - Corning 9863 or 2 mm Schott UG2

B - Corning 5030 + 2 mm Schott GG 13
or 1 mm Schott BG 12 + 2 mm Schott GG 13

V - Corning 3384 or 2 mm Schott GG 11

(b) For photographic observation

U - Kodak 103aO + 2 mm Schott UG2

B - Kodak 103aO + 2 mm Schott GG 13

V - Kodak 103aO + 2 mm Schott GG 11

In photographic photometry it is essential that standard sequences are set up photoelectrically right in the region being investigated. The magnitudes of other stars in the field are then interpolated between those of the photoelectric standards. This minimises errors in transferring zero-points from one part of the sky to another.

To determine the conversion equation Johnson, Morgan and their co-workers have published lists of a variety of standard stars as follows:-

(1) Johnson H.L. & Morgan, W.W. - Astrophysical Journal 117, 313, 1953.

(2) Johnson, H.L. - Ann d'Astrophysique 18, 292, 1955.

(3) Johnson, H.L. & Harris - Astrophysical Journal 120, 196, 1954.

Photoelectric sequences have also been measured for stars in the E-regions in the southern hemisphere; these are convertible

to the U, B, V system within a few hundredths of a magnitude (Cape Mimeograms Nos. 1-5).

Colour-colour relation

The U, B, V system provides two colour-indices; (B - V) which is determined by the colour temperature and (U - B) which describes the Balmer absorption. Bonsack et al. (1957) have obtained expressions for (B - V) and (U - B) in terms of the fluxes effective on the receiver. They have considered $I(\lambda)$ at the respective equivalent wavelengths to be a function of temperature and electron pressure and have expressed the fluxes as ratios of $\frac{I(\lambda)}{B(\lambda)}$, $B(\lambda)$ being the Planck function at the corresponding wavelength. The flux in the ultraviolet band has been taken as the sum of two fluxes at equivalent wavelengths to the shorter and longer wavelength sides of the ultraviolet band. Corrections are applied for individual Balmer lines in the blue band and unresolvable Balmer lines near the series limit in the ultraviolet band.

The normal (unreddened) relation between (U - B) and (B - V) will be different for various groups of stars for the following reasons:

(1) the difference in the relative energy distribution in the continuum in the three spectral regions. For example, early type supergiants have greater ultraviolet radiation than normal main sequence stars of the same colour.

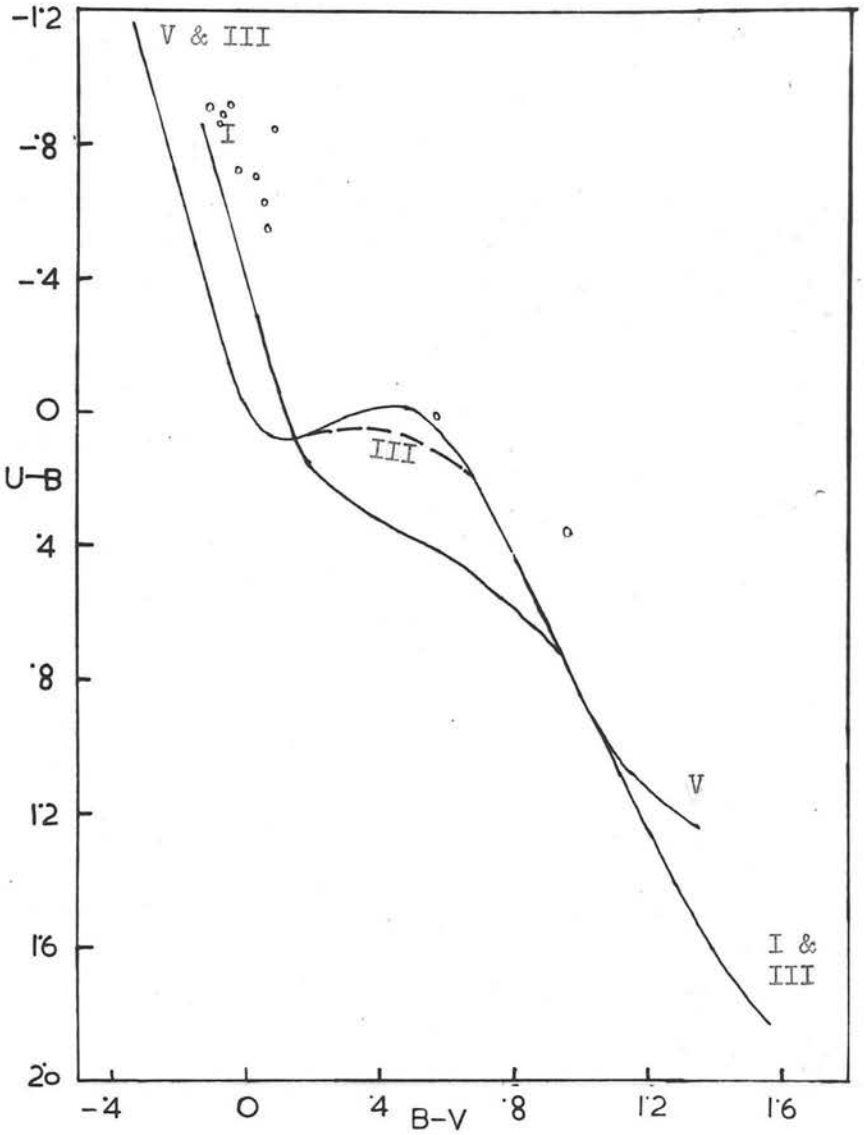

FIG. 2 - Unreddened (U-B, B-V) - diagram for different luminosity classes and white dwarfs. Data from Johnson and Morgan (1953) and Johnson (1958); U-B and B-V colours of white dwarfs from D. L. Harris (Ap. J. 124, 665, 1956).

(2) the blanketing effect, which depends on the distribution and strength of the absorption lines and causes a depression of the continuum in the ultraviolet for stars with large metal content. Stars with an abnormal abundance ratio of hydrogen to metals may be expected to deviate from the (U - B) and (B - V) relation valid for stars with normal metal content.

For cool stars the metal abundance is an important factor in determining the coefficient of absorption and the electron pressure. For hot stars, however, the electron pressure is due to the ionization of hydrogen and the metal abundance has no effect.

The observed relations (unreddened) between (U - B) and (B - V) for different luminosity classes are shown in Figure 2. The depression in (U - B) is a maximum at about spectral class A0, which is due to the large amount of energy absorbed in the hydrogen lines at the limit of the Balmer series. For early type supergiants the curve lies above that of the main sequence. After G0, the relations for all luminosity classes come close together. White dwarfs near (B - V) = 0 are observed to have a large ultraviolet excess. The same systematic excess is observed with late type white dwarfs.

Becker and Steinlin (1956) believe to have shown that if one of the three magnitudes is at longer wavelength, late type stars having known or equal reddening can be separated according to luminosity classes. In Becker's R.G.U. system

the three colours are at equivalent wavelengths 3730A, 4700A and 6380A. Using this system Becker and Steinlin claim to have separated late type unreddened giants from late type unreddened dwarfs. This has been re-examined by Argue (1961) who has concluded that "the R.G.U. system permits one to segregate some, but not all, class III stars of late type from class V."

Interstellar Reddening

Observed apparent magnitudes and colours are affected by interstellar absorption. This absorption is an important factor in the determination of distances by photometric methods. To determine the absolute value of the general absorption is a difficult matter. It is much easier to measure selective absorption, which produces reddening, by determining the spectral type of the star and comparing the observed colour-index with the intrinsic colour-index given by the spectral type-colour index relation. The selective absorption can be converted into total absorption over a given wavelength region, if the relation between the two quantities is known.

It may be assumed that over a wide range of wavelengths the reddening is proportional to λ^{-1} (Whitford, 1958). The ratio of the total to selective absorption can then be calculated from theory and observation. Hiltner and Johnson (1956) comparing reddening on one side of the double cluster h and χ Persei with the reddening on its other side, found

$$\frac{A(V)}{E_{B-V}} = 3.0 \pm 0.2 \qquad (1.13)$$

where A(V) = total absorption in the photovisual magnitude

and E_{B-V} = reddening in (B - V).

There are several determinations of this ratio: Oort derived 3.30, Blanco 3.0.

As regards the uniformity of the law, two regions (the Trapezium region in Orion and the great rift in Cygnus) are believed to have unusual reddening. Even then, the ratio $\frac{A(V)}{E_{B-V}}$ has been found to be about 3.0 (Hiltner and Johnson, 1956).

Thermal reddening does not have the same effect as interstellar reddening on the three wavelength bands. Due to selective absorption, interstellar absorption is relatively greater in the ultraviolet. Choosing suitable wavelengths so that the effect of reddening on the ultraviolet colour-index is equal to that on the blue-yellow colour index, Becker compared the short-wave colour index with the long-wave colour index to give a Colour-Difference (CD). The colour-difference is independent of reddening and shows the deviation from black body radiation. Since this deviation is systematic with spectral type, CD can be correlated with spectral type. This enables one, in theory at least, to recognise the star's intrinsic colour-index from photometry alone. The method would, however, find only a limited application in the case of O and B stars.

For the U, B, V system Johnson and Morgan (1953) have defined a parameter Q, which is similar to CD, by the relation

$$Q = (U - B) - \frac{E_{U-B}}{E_{B-V}} \cdot (B - V) \qquad (1.14)$$

where E_{U-B} = colour excess in U-B,

and E_{B-V} = colour excess in B-V.

This parameter will be free from the effect of reddening. The mean-value for $\frac{E_{U-B}}{E_{B-V}}$ was determined, from the data available for reddened and unreddened B stars, to be ($.72 \pm .03$). By plotting Q against the intrinsic (B - V) for two galactic clusters (NGC 2362 and M36) and for certain selected unreddened bright stars, they have shown that for the given range of Q a straight line is a good representation of the observations.

The equation of the line can be written as

$$(B-V)_{intrinsic} = .337Q - .009, \quad \text{for} \quad -.8 < Q < -.05 \qquad (1.15)$$

This equation can be used to determine the colour-excess for the (B-V) colour-index. The given range of Q limits its application to B type stars of luminosity classes III to V.

For a group of stars whose intrinsic (U - B), (B - V) relation is known, the observed plot of (U - B) against (B - V) can be used successfully to determine reddening corrections. Due to reddening, stars will be shifted in the "colour-colour diagram" along the reddening line. For a cluster, the intrinsic (U - B), (B - V) relation being known for the main sequence stars, the reddening of the cluster can be estimated from the shift of the cluster main-sequence in the observed plot of (U - B) against (B - V).

In the work of Johnson and Morgan the slope of the reddening line has been assumed constant. More recent work by Blanco (1955) and by Hiltner and Johnson (1956) has shown that the reddening line is not straight but curved. They derived the following equation for the reddening line

$$\frac{E_{U-B}}{E_{B-V}} = .72 + .05E_{B-V} \qquad (1.16)$$

Lindholm (1957) has furthermore found that the slope of the reddening line changes with spectral type. The changes will, however, yield relatively minor differences in the results.

The "Q-method" has been recently re-examined by Johnson (1958). Taking account of the systematic changes in the value of $\frac{E_{U-B}}{E_{B-V}}$ with spectral type, he has computed values of Q. The relation between Q and $(B-V)_{int.}$ is given by the equation

$$(B-V)_{int.} = .332Q, \quad \text{for } -.3 \leq B-V \leq 0 \qquad (1.17)$$

This equation (1.17) is slightly different from equation (1.15). It is valid for main sequence stars earlier than spectral type A0.

Determination of Distance

For representation in an H-R diagram, the determination of absolute magnitude requires the computation of the distance modulus of the cluster. The stars in a cluster may be assumed in the first instance to be practically at the same distance. The distance-modulus of a cluster can thus be used to convert all absorption-free apparent magnitudes to absolute magnitudes.

Trigonometric parallaxes are reliable when the distance is less than 20 parsecs. For larger distances the uncertainty increases rapidly. To obtain an accuracy of one-tenth of a magnitude in M (absolute magnitude), an accuracy of about 5 per cent in the distance determination is required.

It is convenient if stars having the same absolute magnitude in all clusters can be recognized by photometric methods. Assuming that the fainter end of the cluster main sequence is unevolved and identical for all clusters and nearby stars, a standard main sequence can be derived, at least in principle, by fitting the main sequence of the clusters for which the geometrical moduli are well known to the main sequence determined from nearby stars. Cluster parallaxes then follow from the fitting of the lower part of the cluster main sequence to the standard main sequence.

Johnson and Morgan (1953) derived a standard main sequence from their photometry of the Pleiades, Praesepe, NGC 2362 and nearby stars. The standard main sequence so derived will,

however, lead to systematic errors in distance moduli of clusters obtained by fitting their main sequences to this standard sequence.

The reason is as follows. The stars of the general field are of different ages and possibly of different origin and, on the average, are much older than the clusters used for standardisation. Now according to Schönberg and Chandrasekhar's theory of stellar evolution (to be described later), the brighter end of the main sequence of a cluster will tend to lie above a main sequence, whose evolution is zero, and stars evolved from the main sequence will be brighter than unevolved stars of the same colour. These effects have been observationally confirmed by Johnson (1954), and Johnson and Sandage (1955).

Consequently, if the main sequence of the Pleiades is fitted to the main-sequence stars of the general field, this fit will yield luminosities too high for the cluster stars, since the Pleiades, being a younger cluster, have evolved less than the main-sequence stars of the general field. Similarly, if the main-sequence of NGC 2362 is fitted to the brighter end of the Pleiades, which is older than the former, the luminosities obtained by this fitting for stars of NGC 2362 will be too high.

To establish a main sequence whose evolution is zero, it is therefore necessary to apply corrections on the basis of the current theory of stellar evolution.

Assuming that the Hyades stars are representative of the main sequence stars in general, Johnson and Knuckles (1955)

derived an "age-zero sequence" by computing evolutionary corrections to the Hyades main sequence on the basis of Harrison's theory (1944). The sequence rests on the well determined parallaxes of the Hyades derived by Van beuren (1952). The "Hyades-basis" was then extended by the use of the Praesepe cluster which led to an age-zero sequence extending from about $B - V = 0.2$ to $B - V = 1.5$ mag.

In a similar manner, Johnson and Hiltner (1956), using the Pleiades main sequence, established the age-zero sequence from $B - V = -.09$ to $B - V = 1.37$. The probable error of this age-zero sequence is estimated to be about $\pm$ 0.2 mag.

Johnson (1957) derived an age-zero sequence from $B - V = -.25$ to $B - V = 1.40$, by piecing together such segments from the Hyades, Pleiades and NGC 2362 as are expected not to have evolved significantly.

The most recent determination of this fundamental sequence is by Johnson and Iriarte (1958) who have bridged the gap between NGC 2362 and the Pleiades, using additional clusters (NGC 2264, NGC 6530, I Per, I Ori, h and χ Per, M36 and M25). Their sequence is estimated to have an accuracy of $\pm$ .1 mag. It differs very little from that derived by Johnson (1957).

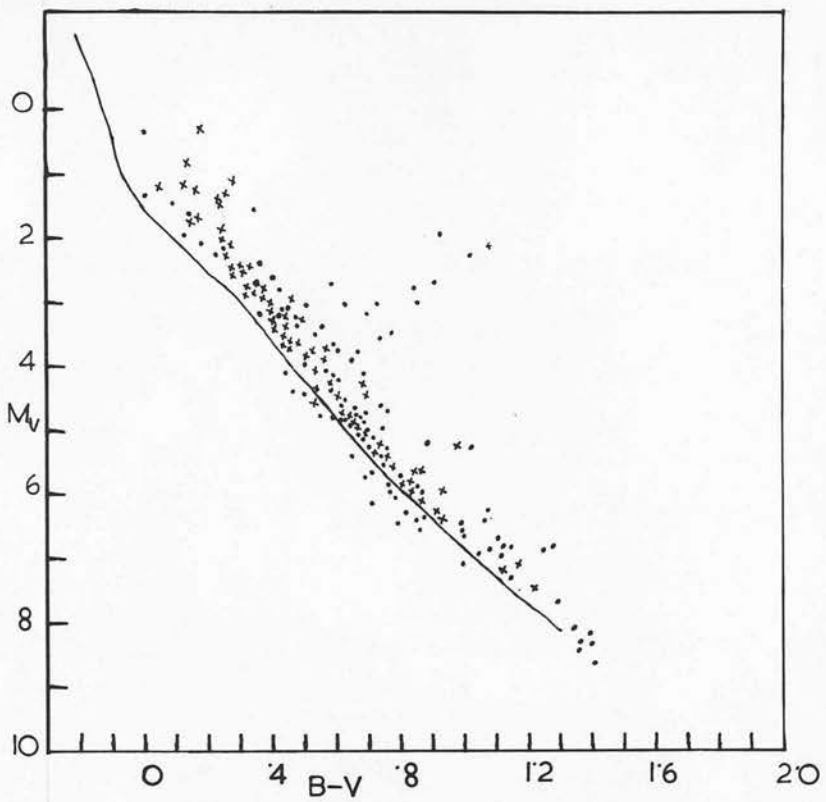

FIG. 3 - Comparison of derived "age-zero sequence" with nearby stars and Hyades. Solid line represents the age-zero sequence; filled circles, nearby stars; and crosses, Hyades stars. Data from Johnson and Morgan (1953) and Johnson and Knuckles (1955).

TABLE I

The standard "age-zero sequence" (according to Johnson and Iriarte).

B - V	Mv	B - V	Mv
- 0.25	- 2.10	0.80	5.88
- 0.20	- 1.10	0.90	6.32
- 0.15	- 0.30	1.00	6.78
- 0.10	+ 0.50	1.10	7.20
- 0.05	+ 1.10	1.20	7.66
+ 0.00	+ 1.50	1.30	8.11
+ 0.05	+ 1.74		
+ 0.10	+ 2.00		
+ 0.20	+ 2.45		
+ 0.30	+ 2.95		
+ 0.40	+ 3.56		
+ 0.50	+ 4.23		
+ 0.60	+ 4.74		
+ .70	+ 5.38		

The accuracy of the derived age-zero sequence is examined in Figure 3.

The diagram represents the nearby stars having known trigonometric parallaxes greater than 0".05, the age-zero sequence and the Hyades. The age-zero sequence coincides with the lower envelope of the nearby stars. The nearby stars appear to deviate from the age-zero sequence near

$M_V = 4.5$. This is in agreement with the hypothesis that the nearby stars are older than the clusters used in establishing the sequence.

The Hyades and the other two sequences merge near $M_V = 5$, which agrees with the theoretical prediction that the stars fainter than $M_V \sim +5$ have hardly evolved from the main sequence. The zero-point of the Hyades and the age-zero sequence is thus confirmed.

Any distance modulus derived by fitting the cluster main sequence to the age-zero sequence contains the following sources of error:

(1) uncertainty in the determination of cluster reddening,

(2) uncertainty in the value of the ratio of total to selective absorption,

(3) uncertainty in the fit of the cluster main sequence to the age-zero main sequence,

(4) the probable error of the age-zero sequence.

On account of these various errors, a derived distance modulus may well be wrong by $\pm$ 0.3 mag.

CHAPTER II

INTERPRETATION OF H-R DIAGRAMS

H-R Diagrams of Open Cluster

A representative sample of open clusters reveals various systematic peculiarities and determines distinct regions in the H-R diagram.

Clusters which are connected with diffuse nebulae contain luminous early type stars. The shapes of the colour-magnitude diagrams of these clusters are very diverse.

Some of these "nebulous clusters," for instance, NGC 2264 (Walker, 1956), NGC 6530 (Walker, 1957), and the Orion Cluster (Parenago, 1954; Johnson, 1957), show unusual behaviour of the fainter end of their main sequences.

The normal main-sequence of NGC 2264 extends from O7 to A0. Beyond A0 there is a group of stars lying above the normal main sequence in the subgiant region. NGC 6530 is very similar to NGC 2264, the main sequence extending from O5 to A0. In the Orion cluster the main-sequence covers the spectral range from O5 to A0. The fainter part ends abruptly. A scattered group of stars of later spectral classes lies above the normal position of the main sequence.

According to Strömgren (1952), the upper limit of the age of these clusters as computed from their brightest stars is of the order of 3×10^6 years.

An interesting feature of these extremely young clusters is that many of the stars fainter than Mv = 3.5 are T Tauri variables which have hydrogen emission lines. The spectra of these T Tauri variables, as well as of some non-variable stars of later type, show broadened lines which may indicate rapid rotation.

NGC 2362 (Johnson and Morgan, 1953; Johnson and Hiltner 1956) contains luminous B type stars. The cluster main sequence extends upwards to great luminosity. Its fainter end appears at the same time to deviate to the right of the age-zero sequence.

The double cluster h and χ Persei (Johnson and Morgan 1955, Johnson & Hiltner, 1956) contains, besides early B type stars, hot giants, red M-type supergiants and emission line stars. The upper part of the main sequence deviates to the right and comes to an abrupt end; at the other side of a wide gap, a sequence of M-type supergiants appears.

In the Pleiades (Johnson and Morgan, 1951; Mitchell and Johnson, 1957) the brightest stars are of late B type. A break in the cluster main sequence is observed at $M_V = 6.5$, $B - V = .90$.

The colour magnitude diagrams of the clusters containing

early type stars differ from those of the clusters containing giants. The well observed clusters belonging to the later group are the Hyades (Johnson and Knuckles, 1955), Praesepe (Johnson, 1952b), M11 (Johnson, Sandage and Wahlquist, 1956), M41 (Cox, 1954) and NGC 752 (Johnson, 1953). Each cluster has a giant branch as well as a main sequence, leaving a gap (the Hertzsprung gap) between the giant sequence and the main sequence. The main sequence begins with A or late type stars. The brightest stars in all these clusters are less luminous than those in the Pleiades.

The colour-magnitude diagrams of M67 (Johnson and Sandage, 1955) and NGC 188 (Sandage and Van den Bergh, 1960) are quite different from those of other open clusters. There is no Hertzsprung gap; there is a subgiant sequence, an upward extension of the main sequence which continues up to the giant branch; and the giants have a large range of luminosity. A group of blue stars appears on the main sequence.

To obtain a composite H-R diagram of this sample of clusters, Sandage (1957a) fitted their observed cluster main-sequences to a standard sequence which he derived empirically by fitting together the portions of the main sequences of various clusters which lie about 3^m below the brightest main sequence stars. He assumed that in this region effects of evolution in the colour-magnitude

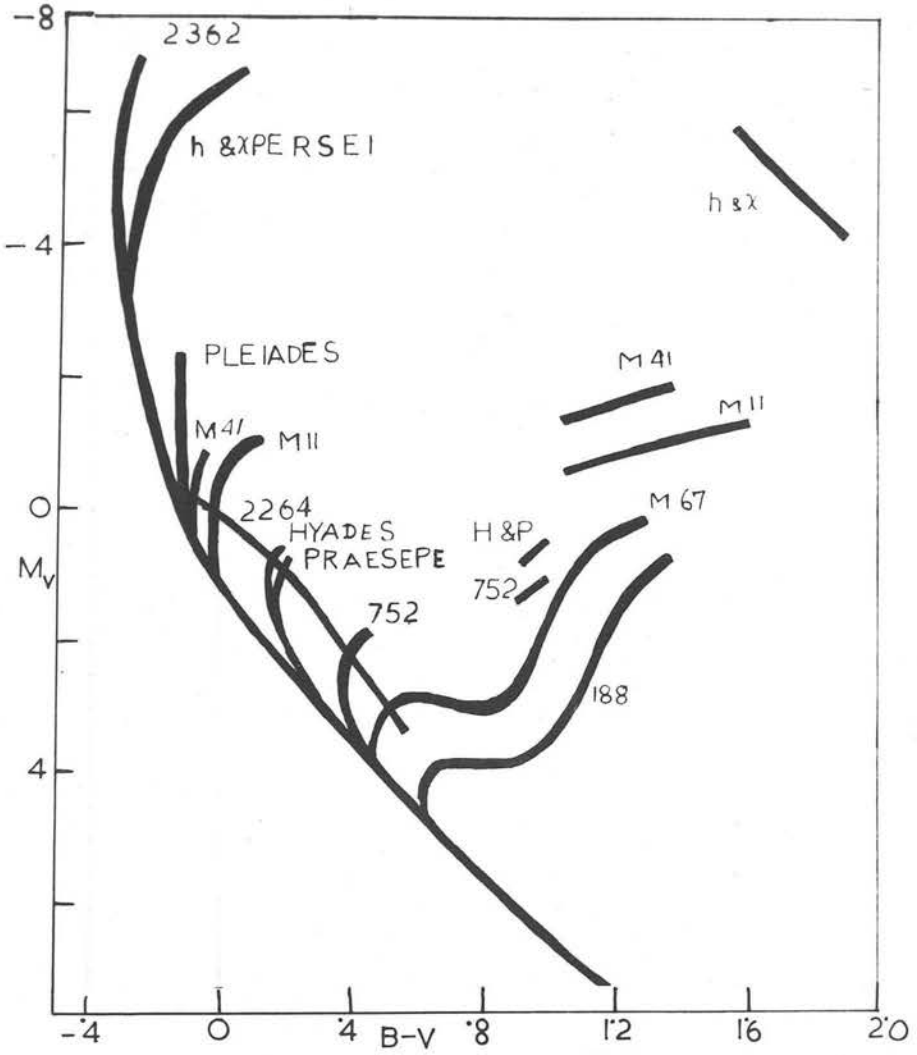

FIG. 4 - Composite H-R diagram for 11 galactic clusters. Adapted from a diagram by Sandage.

diagram may be neglected. The stars of his standard sequence are about 0.2 mag. brighter than those of Johnson's age-zero sequence. For the comparative study of clusters this difference is, however, negligible.

Of all the characteristic features of Sandage's diagram (Figure 4) the most important one is the turn-off of the cluster main-sequences to the right of the standard sequence. The bright ends of the main sequences for different clusters deviate at different absolute magnitudes. In young clusters (like NGC 6530, NGC 2362) the lower part of the main sequence is shifted to the right. The diagram shows clearly the Hertzsprung gap which is widest in those clusters whose main sequences extend furthest upwards. The beginning of the Hertzsprung gap occurs at about $M_v = 2$. The luminosities of the giants are nearly the same as the luminosities of stars at turn-off point on the main-sequence. The gap disappears at about $M_v = 4$.

An important feature of the giant sequences is that they appear to converge in luminosity toward red colour indices. Sandage has called this the "funnel effect".

The presentation of an evolutionary picture from these features, however, requires the assumption that all the regions of the H-R diagram, which can be occupied by the galactic clusters in general, have been determined.

This can be examined by comparing this composite diagram with the H-R diagram of general field stars. The

stars in the general galactic field are expected to represent a mixture of stars of different origin and different ages. The combined H-R diagram of the maximum possible numbers of star clusters should approach in form the H-R diagram for stars in the general field.

By superimposing the stars within 15 parsecs of the Sun on the composite cluster diagram, Sandage (1958a) has shown that the stars mostly lie in the regions occupied by the galactic clusters chosen for the diagram.

Contraction Hypothesis

The history of a star at the time before it reaches the main sequence is least well known. It is assumed that the first stage of evolution of a star is the Kelvin Contraction stage, gravitational energy released by contraction being the source of energy. Half of this energy is radiated and the remaining half raises the central temperature. This phase lasts till the central temperature is sufficient to start nuclear interactions.

Evolutionary tracks in the bolometric magnitude - effective temperature plane have been computed for model stars of different masses by Henyey et al. (1955). The assumptions for the models are that (1) mass and chemical composition do not change, (2) perfect gas equation holds good, (3) there is no convection core, since the energy generated is spread throughout the star, (4) models contract homologously. Thomas (1931) has shown that for homologously contracting models Kramer's opacity law is obeyed and that the ratio of the two specific heats, $\gamma = \frac{5}{3}$.

Sandage (1958b) has obtained an approximate equation for the track in the form

$$\triangle(M_{Bol.}) = - 2 \triangle(\log Te) \qquad (2.1)$$

Luminosity increases slowly as the surface temperature increases rapidly so that the star approaches the main sequence from the right. One peculiarity in these theoretical tracks is that

they attain a maximum just before they reach the main sequence, at a point when hydrogen burning starts. The contraction then becomes slower, reducing the rate of gravitational energy release. Nuclear burning, however, is not sufficient to compensate for this deficit. The thermonuclear source replaces the gravitational source in a smooth transition.

An estimate of the contraction time scale from radius R_o, given by the initial configuration, to radius R is obtained as follows.

The internal energy U of the gas sphere is given by

$$3(\gamma - 1)U + \Omega = 0, \quad \Omega \text{ being the potential energy} \qquad (2.2)$$

(S. Chandrasekhar - An Introduction to the Theory of Stellar Structure, p. 52, Chicago University Press, 1939).

On contraction, Ω is decreased by $\Delta\Omega$, say. The gain in the internal energy is then

$$\Delta U = -\frac{1}{3(\gamma-1)} \Delta\Omega \quad , \qquad (2.3)$$

the fraction,

$$\frac{3\gamma - 4}{3(\gamma-1)}$$

being radiated.

Therefore the luminosity L is given by

$$L = -\frac{3\gamma - 4}{3(\gamma-1)} \cdot \frac{d\Omega}{dt} \qquad (2.4)$$

For a configuration of polytropic index n,

$$\Omega = \frac{3}{5-n} \cdot \frac{GM^2}{R} \qquad (2.5)$$

where M is the mass and R the radius.

Then $$L = -\frac{3\gamma - 4}{\gamma - 1} \cdot \frac{1}{5 - n} \cdot \frac{GM^2}{R^2} \cdot \frac{dR}{dt} \qquad (2.6)$$

So that if the mass and chemical composition remain constant

$$\frac{dR}{dt} \propto (LR^2) \qquad (2.7)$$

If the star had existed with a mean luminosity $\bar{L}$, i.e. ignoring that the luminosity is a function of the radius, the time to contract from R_o to R is

$$t = \frac{3\gamma - 4}{\gamma - 1} \cdot \frac{1}{5-n} \cdot \frac{GM^2}{\bar{L}} \left(\frac{1}{R} - \frac{1}{R_o}\right) \qquad (2.8)$$

For $R_o \gg R$,

$$t = \frac{3\gamma-4}{\gamma-1} \cdot \frac{1}{5-n} \cdot \frac{GM^2}{\bar{L}.R} \qquad (2.9)$$

But as the star contracts, its luminosity changes with radius. The mass-luminosity composition relation for a star with Kramer's opacity can be written as

$$L = \text{Const.} \frac{M^{5.5}\mu^{7.5}}{R^{\frac{1}{2}}} \qquad (2.10)$$

where μ is the mean molecular weight.

For constant mass and chemical composition

$$L \propto R^{-\frac{1}{2}} \qquad (2.11)$$

From equation (2.6) the time to contract from an infinite sphere to the dimensions of main-sequence stars is

$$t_{g,c} = 2 \times \frac{3\gamma-4}{\gamma-1} \cdot \frac{1}{5-n} \cdot \frac{GM^2}{L_{MS} \cdot R} \qquad (2.12)$$

where L_{MS} is the main-sequence luminosity of the star.

Levee (1953) has shown that for a contracting model $n = 3$ is a good approximation and that the total time taken by the Sun for gravitational contraction is 5.04×10^7 years. When mass, radius and luminosity are expressed in solar units, the equation (2.12) can be written as

$$t_{g,c} = 5.04 \times 10^7 \frac{M^2}{L_{MS} \cdot R} \text{ years} \qquad (2.13)$$

Nuclear burning of D, Li, Be or B may occur and increase the contraction time by the order of $\frac{E_N}{L}$ seconds, where E_N is the energy released by the nuclear burning. The equation (2.13) shows that massive stars will reach the main sequence much more rapidly than less massive stars. For young clusters, stars whose parameters are large enough for $t_{g,c} \lesssim \tau$, the age of the cluster, are on the main sequence. Stars fainter than these are still in the process of contraction.

An observational test of this hypothesis is that, in colour-magnitude diagrams of young clusters, the lower ends

of the main sequences should turn off at a critical luminosity given by $t_{g,c} = \tau$. Such a test was first suggested by Salpeter (1953).

These ideas seem confirmed by observation of colour-magnitude diagrams of NGC 2264, NGC 6530, I Orionis and NGC 2362. The faint members of these clusters are more luminous than main-sequence stars of the same colour; they have been interpreted as stars which are still in the process of contraction.

Sandage (1958b) has compared Walker's observations on NGC 2264 and NGC 6530 with theoretically predicted tracks of evolution. The ages determined from the upper end of the main sequence and the contraction time for an A0 star are both of the order of 3×10^6 years. However, a difficulty arises as regards the time-scale for the evolution of the fainter stars. A period of 3×10^6 years seems too short for the fainter stars to have contracted to their observed positions.

Herbig has pointed out (during the discussion when Sandage presented his paper) that T Tauri stars with emission lines appear bluer than normal stars having the same spectral type; the normal relationship between (B - V) and Te may not be applicable to these stars.

Taking this into account Varsavsky (1960) has used Joy's data in the Taurus clouds. Having found an error in the computed tracks he has computed anew the theoretical colour-

magnitude diagram for a cluster 3×10^6 years old, based on the work of Henyey et al. It has been shown that the computed colour-magnitude diagram is in good quantitative agreement with the observed ones. There is, however, a discrepancy in the case of very red stars. This may be due to the large uncertainties in the bolometric corrections, or to the theory which may be too simple. The theory may well be improved by more observations on very young clusters. Cox (1960) and his associates, allowing for convection in the model have computed contraction paths which are lower than the previous ones.

Observationally, the uncertainties are largest for the faintest stars. Miss Underhill (1960) has wisely pointed out that the fainter "cluster" stars and the lower end of the main sequence may well be confused with field stars.

Due to theirirregular light variations, it is difficult to identify the intrinsic position of T Tauri stars in colour-magnitude diagrams.

Variable absorption within the cluster may also cause some uncertainty in the determination of absolute magnitudes.

However, there are indications that the turn-off point at the faint end of the main-sequence really differentiates the main sequence stars from a contracting phase. Mitchell and Johnson (1957) are certain that in the Pleiades there are some stars in the contraction stage. The lower turn-off

occurs near $M_V = 6.5$, thus lying about 9 magnitudes below the brightest star observed in the cluster. This observation confirms Von Hoerner's (1957) prediction that in any cluster the total range of the main sequence should be about 9.5 bolometric magnitudes.

Initial Main Sequence ("age-zero" sequence).

The initial main sequence represents the locus of stars in which hydrogen nuclear burning provides the source of energy, but in which nuclear processes have not yet had time to cause any chemical inhomogeneities.

The structure of main sequence stars depends on the dominant energy-producing process and on the form of the opacity law, both of which are determined by the central temperature. Energy generation rates recently given by Fowler (1960) show that for masses below 1.3 $M_\odot$, the p-p reaction dominates and above this the C-N cycle dominates, but for masses $M_\odot < M < 3M_\odot$ both processes are important.

For stars burning on the p-p chain, the energy flux in the core does not reach large values so that the radiative temperature gradient will not be very steep. Hence the core is in radiative equilibrium. However, the transport of energy is not radiative throughout. Models assuming radiative equilibrium throughout indicate either high luminosity or low hydrogen content. Osterbrock (1953), following Unsöld (1938), Biermann (1938), and Strömgren (1952), has pointed out that a convection zone in the envelope may affect the interior structure. Although the very outermost layers are in radiative equilibrim, the

opacity increases inward due to the ionization of hydrogen and the radiative gradient becomes too steep for stability. As a result, a convection zone develops. This zone begins in the lower photosphere and extends inward to a considerable depth. In a convective zone the temperature gradient is less than in a radiative one. If the existence of an atmospheric convection zone is taken into account, the central temperature of the corresponding star will have a lower value than if the star were radiative throughout.

For stars deriving their energy from the CN cycle, energy production is concentrated in the centre of the star. The corresponding temperature-gradient at the centre is steep enough to produce a convective core. The size of this core increases with the mass of the star.

When both processes are in operation, energy production by the p-p chain occurs outside the core in which the CN cycle operates, and the energy-producing area becomes extensive in this case. The existence or non-existence of a convective core is determined by a criterion established by Naur and Osterbrock (1953).

The initial main sequence is well defined for a star of pure hydrogen. The question arises which is the influence on its position in the H-R diagram of a somewhat different original composition. Reiz (1954) was the first to investigate this problem. His model stars range over masses from .7 to 1 $M_\odot$, and he assumes that stars burn on

the p-p chain and are in radiative equilibrium throughout. He finds that metal deficient stars initially lie below a "normal" main sequence, in which a certain abundance of metals is assumed.

Hoyle and Haselgrove (1959) have computed the initial main-sequence for two compositions

$$X = .75\ , \quad Y = .24, \quad Z = .01$$
$$X = .99\ , \quad Y = .009, \quad Z = .001\ ,$$

where X, Y, Z denote the abundance of hydrogen, helium and all the heavier elements, respectively. The difference between two sequences is about .25 mag.

Taking account of the atmospheric convection zone Demarque (1960) has shown that the shift does not exceed a few tenths of a magnitude even in cases of extreme metal deficiency. The result agrees with recent observations of Sandage (1958a), that subdwarfs, which are believed to be metal deficient, lie close to the normal main sequence in the M_{Bol}, log Te plane after correcting for line blanketing.

Thus theoretical considerations show that the "age-zero main sequences" are in fact nearly identical in all clusters and in the case of solar-neighbourhood stars, and that the main sequences of several clusters in general can be legitimately fitted together.

Initial Evolution

Due to the transmutation of hydrogen into helium, there must be changes in chemical composition where nuclear reactions take place. A number of possibilities can be considered:-

(1) The star remains homogeneous through complete mixing between core and envelope and the mass remains constant.

(2) Mixing takes place between core and envelope but at the same time the star ejects mass at a steady state.

(3) No mixing takes place between core and envelope and the mass remains constant.

A preliminary investigation shows that if a star remains well mixed throughout, the mass remaining constant, pressure will decrease everywhere due to the increase in mean molecular weight, at a given temperature.

The luminosity, radius and temperature are given by

$$\frac{R}{R_0} = \left(\frac{\mu}{\mu_0}\right)^{0.286}, \quad \frac{L}{L_0} = \left(\frac{\mu}{\mu_0}\right)^{8.06}, \quad \frac{T_e}{T_{e_0}} = \left(\frac{\mu}{\mu_0}\right)^{1.87} \qquad (2.17)$$

where the zero subscript refers to the initial state.

(Schwarschild - Structure and Evolution of Stars, p. 173, Princeton Univ. Press, 1958).

This shows that as the star contracts, the energy-generation rate increases and the star becomes more luminous and bluer. In the colour-magnitude diagram the star moves up and to the left of the main sequence.

The theory considering the second possibility is due to Fessenkov (1952), and subsequently developed by Massevich, Parenago and others. This theory proposes that a star remains homogeneous at all times and evolves down the main sequence ejecting mass at a rate proportional to luminosity. The postulate of mass-ejection through corpuscular radiation becomes necessary so that all stars satisfy a M-L relation of the form,

$$\log L = 4 \log M + \text{constant} \qquad (2.18)$$

The rate of mass loss is given by

$$\frac{dM}{dt} = - .07\, L, \qquad (2.19)$$

M and L being measured in solar units and t in units of 10^9 years. Ejection becomes insignificant when the star reaches the region of the Sun in the mass-luminosity diagram. The star remains in this stage for a considerable period while mixing is negligible. The star leaves the main sequence when a limit, similar to the Schönberg-Chandrasekhar limit, is reached.

According to this theory, the differences in the colour-magnitude diagrams of different clusters can be explained by each cluster having a different composition.

The luminosity function predicted on the basis of mass-loss theory is in good agreement with the observed general luminosity function.

The objections against the mass-loss theory are

(1) There is no observational evidence that the rate of any loss of mass is proportional to luminosity. The loss computed for the Sun would be about .07 $M_\odot$ in 10^9 years, a very high value.

(2) More serious even is the assumption about mixing. The mechanisms capable of mixing are convection and rotation. In a convective region mixing is fairly rapid. Convection in a core can, however, never reach the envelope, unless the star is convective throughout. The evolution of such stars is so slow, however, that their evolution has no practical significance.

Milne (1923) and Zeipel (1924) have shown that in a rotating star, the composition of which is homogeneous at the equipotential surface, radiation alone cannot maintain thermal equilibrium. As a result, currents arise in planes through the axis of rotation. The time taken by such a meridional current to transport material from the core to the surface, as investigated by Sweet (1950) is given by

$$t_m = 3{\cdot}2 \times 10^{13} \cdot L^{-1} \cdot M^{3} \cdot R^{-2} \cdot v^{-2} \text{ years} \qquad (2.20)$$

where v_{rotation} is the equatorial velocity; L, M and R are measured in solar units; v is expressed in Km/sec.

It can be shown that for stars of type later than F, rotational currents are too slow to produce any effective

mixing. Strömgren (1952) has estimated that the massive Oe and Be stars which have high rotational velocities are well mixed. The following consideration renders the condition for mixing even more stringent. It was pointed out by Mestel (1953) that, as any circulation current sets in, heavy materials will rise upwards along the axis of rotation. He has shown that the inhomogeneity in the equipotential surface will tend to choke the circulation, and retard the mixing time. It thus appears that the assumption of mixing in the initial state is far from true for the majority of stars.

In the theory originally proposed by Schönberg and Chandrasekhar (1942) and later extended by Sandage and Schwarzschild (1952), the third possibility is considered. With the gradual conversion of hydrogen to helium, the central regions will have a greater molecular weight. Because of turbulent mixing the core remains well mixed, but an inhomogeneity develops between the core and envelope. When the fuel in the core is exhausted, the convection stops, for there will be no further energy production in the core and no temperature gradient is necessary to transport energy outward. The helium core thus becomes isothermal. Energy is now produced in a thin shell surrounding this isothermal core. When hydrogen in this shell is exhausted, the shell becomes isothermal and the energy producing region moves outwards. Thus the helium core grows. Schönberg and

Chandrasekhar have shown that for a given $\frac{\mu_c}{\mu_e}$, there is a limit to the mass of the isothermal core beyond which equilibrium is not possible. This critical mass of the isothermal core is known as the Schönberg-Chandrasekhar limit. Sandage and Schwarzschild (1952) have proved that this limit is reached when 12% of the mass of the star has become hydrogen exhausted. When this occurs, the structure of the star changes very rapidly and the star leaves the main sequence, moving to the right in the colour-magnitude diagram. The evolving star at first remains close to the main sequence till it becomes about 1.4 mag. brighter when it abruptly leaves the vicinity of the main sequence.

In the Sandage-Schwarzschild model it has been assumed that the inhomogeneity develops discontinuously, which requires that either the helium core grows, or the interface between core and envelope remains at a fixed layer. In massive stars the convective core is much larger than the Schönberg-Chandrasekhar limit and electron scattering is dominant. In such stars the mass fraction in the convective core shrinks as the evolution proceeds. Consequently, between the core and the envelope, there will be an intermediate zone. The layers of the intermediate zone were initially inside the core and its composition is determined by the time when it leaves the core. The outer layers of this zone remain inside the core for a shorter time than the inner layers. So there will be a continuous gradation of composition.

Taylor (1954) and Kushwaha (1957) have considered models taking account of this intermediate zone. The mode of evolution according to these models is that as hydrogen is consumed in massive stars, they move slowly to the right of the main-sequence, their luminosities increasing very little. Kushwaha has computed tracks on this model for masses $10M_{\odot}$, $5M_{\odot}$ and $2.5\ M_{\odot}$, representing the initial stage of evolution. The three tracks are similar in form except that in the case of most massive stars the track begins to move back towards the main sequence. It has been shown that the tracks agree with the observed main sequence in this mass range.

The extent of the intermediate zone is strongly dependent on the law for the absorption coefficient. When Kramer's opacity holds, this intermediate zone is negligible.

The Schönberg-Chandrasekhar theory explains well the behaviour of the main sequence at its upper determination point in the H-R diagrams of the galactic clusters.

Dating of Clusters

The time to reach the Schönberg-Chandrasekhar limit depends on the stellar mass. The energy source of a star of a given composition is proportional to its mass, while its luminosity varies as its mass is raised to a power greater than one. Therefore a massive star consumes the initial energy supply faster than a less massive star and therefore evolves away more quickly. In a cluster the stars which have consumed the critical fraction of hydrogen leave the main sequence while the remaining stars stay on the main sequence. So the turn-off point of the cluster (the brightest main sequence star) can be identified with the stage when the star has reached the limiting core-mass. This provides the method for deducing the ages of clusters.

From the Sandage-Schwarzschild model Sandage (1958c) has obtained

$$\tau = 1.1 \times 10^{10} \cdot \frac{M}{L_T} \text{ years} \qquad (2.21)$$

where τ = age of the cluster reckoned from the initial main sequence state,

M = mass of an evolving star just leaving the main sequence measured in solar units.

and L_T = luminosity at the termination point expressed in solar units.

According to equation (2.21) the order of the age of the clusters is obtained by arranging them in the order of the luminosities at their respective termination points. Sandage derived absolute ages by fitting the cluster main sequences to his empirical age-zero sequence.

The expression (2.21), however, is only approximate. The critical core mass for the Schönberg-Chandrasekhar limit has been assumed by Sandage to be independent of mass. In Taylor's model for a massive star it has been shown that the star may not have reached the isothermal core condition even when 20% of the mass has been converted to hydrogen. Sandage's assumption of homologous models for the stars of younger clusters may not be true. For very faint stars the models may not be homologous. The extent of the initial rise of the star up the main sequence as it goes to the Schönberg-Chandrasekhar limit is an important factor in determining absolute age.

The turn-off point of NGC 188 yields approximately an age of 20×10^9 years. This very long time scale raises the question, as Oört pointed out (in the discussion of Sandage's paper at the Vatican Conference, 1957), whether it is possible for any galactic cluster to withstand the tidal distortions from gravitational sources for longer than 5×10^9 years.

Evolution off the Main Sequences

The evolutionary developments after the stars have reached the limiting core mass depend critically on the mass of the stars. Since the density of the massive stars (heavier than about 1.3 solar masses) is low, the isothermal helium core remains non-degenerate, in which case the ideal gas law holds. Such a core cannot support the pressure of the upper layers and consequently the core begins to contract, releasing gravitational energy. Schwarzschild (1958) has shown that when a star has a gravitationally contracting core and a shell source of nuclear energy, its envelope expands by a factor of 3, its effective temperature falls by about40%, but its luminosity changes very little. Therefore the star for the first time makes a rapid evolutionary movement to the right in the colour-magnitude diagram, close to a line of constant luminosity. The temperature in the core is raised by the energy released by the contraction. When this temperature is sufficiently high to start helium burning, the contraction of the core stops, the rate of expansion of the envelope slows down, and the star cluster finds itself in the giant region of the H-R diagram. When the external layers become sufficiently extended and cool, the formation of an outer envelope zone may halt the expansion.

For less massive stars (less than 1.3 solar masses) the contraction of the core does not begin as soon as the isothermal

condition is reached. The density of the core is high enough so that degeneracy occurs. There will be an extensive growth of a partially degenerate isothermal helium core with a steady increase in the extent of the envelope. Increase in the average molecular weight in the star will cause a continuous increase in the luminosity. The formation of a convection zone below the photosphere extending into the interior to a considerable depth will, however, lessen the expansion. When the luminosity has increased by a factor of about a thousand compared with the main sequence stage, the core contracts sufficiently fast to maintain a temperature-gradient between the centre and boundary of the core, and raises the central temperature high enough for helium burning to begin. When helium burning starts, the central temperature increases rapidly until the core becomes non-degenerate. Non-degeneracy acts as a "safety valve". If there is any increase in the energy production, the temperature rises. Consequently the pressure increases and the envelope expands. The expansion of the envelope leads to a cooling. Energy production, being sensitive to temperature, decreases. Through this natural balancing process between energy generation and energy outflow the star adjusts itself to a stable configuration. So the star ceases to ascend the giant branch when the core becomes non-degenerate. This model, which is due to Hoyle and Schwarzschild (1955), describes the evolution of less

massive stars along the subgiant branch and up towards the giant branch.

The time-scale for traversing these evolutionary tracks beyond the Schönberg-Chandrasekhar limit is very short, relative to the time spent on the main sequence. In the the observed H-R diagram of a cluster the evolving stars in the giant region have come from a small mass range of the main sequence; they represent the track of a star whose mass is a little greater than that corresponding to the upper turn-off point of the main sequence.

The tracks computed for stellar masses of 1.1 and 1.2$M_{\odot}$ by Hoyle and Schwarschild, and Haselgrove and Hoyle (1956) are in reasonable agreement with observation.

According to this scheme of evolution stars can pass through the giant region in two ways - as young, heavy stars evolving straight from the main-sequence without much change in luminosity, or as old stars of nearly solar mass, moving up from fainter regions of the main-sequence. This explains the observed "funnel-effect".

Consequently, a spread in mass may be expected among giants of luminosity class III. Sandage has estimated that about 70% of these giants are of near solar mass, while about 30% lie near to the main sequence M-L relation. The kinematical behaviour of K III giants in the solar neighbourhood shows that nearly 70% move like F stars whilst the others move like A stars, confirming the above.

Mass Ejection

There is some observational evidence that stars in the supergiant and giant regions eject mass. Direct evidence comes from π Pegasi of type F5II - III, the supergiant P Cygni of type B1 and the M type supergiant which is a component of α Hercules.

A general argument comes from the investigation of galactic clusters like M67. In the colour-magnitude diagram of M67, a few stars are observed on a horizontal branch subsequent to the tip of the giant branch. Sandage (1957b) has obtained a method to determine from the observed luminosity function the evolutionary tracks for the stars of M67, and to estimate the times spent by a star at each luminosity. Now if the star spends a time interval Δt with a luminosity L, the amount of hydrogen burnt is given by

$$L \cdot \Delta t = \cdot 007 c^2 \cdot x \cdot \Delta q \cdot M \qquad (2.22)$$

where x = initial hydrogen concentration, and
where Δq is the fraction of hydrogen that is burnt.

Summing over each interval it is estimated that the star spends about 60% of its initial hydrogen content to reach the extreme left of the horizontal branch. It is believed that these stars are nearing the end of their lives. So the remaining 40% of its hydrogen fuel remains unaccounted for. It is possible that some hydrogen may be lost during the giant phase of evolution.

The general effect of mass loss is to speed up the normal evolution of the star. The estimated rate of mass loss in α Herculis is about 10^{18} g/sec. The physical processes that are responsible for mass loss are not theoretically understood. The obvious condition for mass ejection is that the mechanism must produce a mechanical energy flux to provide the kinetic energy for escape. Radiation pressure does not seem a possible mechanism to eject mass at the rate at which α Herculis is losing mass.

One possible mechanism, as assumed by Biermann (1948) and Schwarzschild (1948) is that high turbulence in the photosphere of red giants acts as a source of acoustic waves. These acoustic waves represent a mechanical energy flux which may be sufficient to account for the rate of ejection. From spectroscopic observations it is known that turbulent velocities in the photosphere of a red giant is very high, about five times greater than in the Sun.

Hoyle (1956) has suggested that in a late type giant like α Herculis the ionization energy of the material in the convective zone may be an effective energy source. But how this ionization energy is converted into kinetic energy is not clear.

Fast rotation may be responsible for mass ejection in some giants, as in the case of π Pegasi (Greenstein, 1953).

Mass loss may also occur from the effects of hydromagnetic processes. This possibility has been discussed by Biermann (1955).

Effect of Chemical Composition

During the phase with a large helium core, the evolutionary behaviour of the giant star depends on its metal content. The theoretical models of Hoyle and Schwarzschild (1955) show that the giant branch for stars having relatively low metal content is brighter than that for stars with the metal abundance which we find in the Sun.

M67, as an old galactic cluster, may now be compared to the globular clusters. Distinct differences in the colour-magnitude diagrams of two kinds of clusters can be demonstrated by comparing M67 with M3. The main sequences of both clusters turn off at about the same point, which implies that they cannot differ much in age and that the evolving stars have approximately equal masses. But the giant branch of M67 is much flatter than that of M3. The parameter responsible for this difference in their colour-magnitude diagrams is likely to be chamical composition. The observed difference between M67 and M3 is similar to that predicted by Hoyle and Schwarzschild if M67 has a higher metal content than M3 by a factor of 15.

The following observations also indicate that the chemical compositions of galactic and globular clusters are probably different.

(1) Most of the nearby stars known to be in galactic clusters have normal spectra with strong metallic lines.

In contrast spectra available on globular cluster stars show weakness of the metallic lines.

(2) The members of globular clusters show an ultraviolet excess which varies from cluster to cluster. Ultraviolet excess has been interpreted as a measure of the under-abundance of metals (Arp, 1959).

Recent observations of Sandage and Wallerstein (1960) also show that the positions of the giant sequences in clusters depend on metal abundances. They have compared the colour-magnitude diagrams of M92, M3, NGC 6356 and M67: M92 and M3 are halo globular clusters with very low metal abundance; NGC 6356 is a disc globular cluster with a relatively high metal abundance; and M67 is an old galactic cluster, yet its chemical composition is the same as that of young solar-neighbourhood stars.

The giant sequences of these clusters lie systematically at higher absolute magnitude as the metal content decreases.

Though much theoretical work has yet to be done to determine the evolutionary tracks of giants for a wide range of chemical compositions, all these observations suggest that

(1) there is a continuous gradation of heavy element content in stars,

(2) stellar population characteristics are correlated with the chemical composition of stars, and

(3) the giant branch in the colour magnitude diagram gives information about stellar population.

Advanced Stages of Evolution

The difficulty in tracing evolutionary effects after the stars have left the giant region of the H-R diagram is that galactic clusters do not contain enough stars. Globular clusters, however, provide some clues to advanced stages of evolution. The structure of stars at advanced evolutionary stages is very imperfectly understood. A schematic evolutionary picture is as follows:-

Subsequent to the giant branch there appears a well populated sequence of stars forming the horizontal branch in the colour-magnitude diagrams of globular clusters. In M67 a sparse distribution of stars is observed, which looks rather similar to the horizontal branch stars in globular clusters. Possibly the horizontal branch represents an evolutionary locus of stars of masses near $1.2M_{\odot}$ subsequent to the red giant phase. Perhaps because of a change to helium burning or of a mass loss, stellar conditions change suddenly and as a result the star's luminosity is lowered. This means that the track again runs from right to left in the H-R diagram. The stars may attain a stable structure whose locus is defined by the horizontal branch. After some time, the stars may again become unstable, move off the horizontal branch, and descend rapidly to the white dwarf region. A number of factors may determine the course of evolution.

(1) contraction of the core

(2) rotation

(3) gradual ejection of mass

(4) catastrophic ejection of mass.

Since there is an upper limit to the mass of a white dwarf, a star exceeding this mass must undergo some mass loss before becoming a white dwarf.

Extension of the Main-Sequence

In the H-R diagram of old clusters like M67, M3 (Sandage, 1953), NGC 7789 (Burbidge & Sandage, 1958), a thinly populated sequence of stars lies more or less on the main sequence above the turn-off point. A possible interpretation of these blue main-sequence stars is that either

(1) these stars have evolved as homogeneous stars, or that

(2) the stars have been formed relatively recently.

It is very unlikely that in a cluster some members evolve homogeneously, while other members are evolving inhomogeneously, as (1) requires.

(2) requires the presence of interstellar matter within the cluster. This matter can hardly be the remains of original dust and gas since these must have been swept away when the cluster travelled across the galactic plane. The matter might have been released within the clusters during

supernovae explosions of the massive stars. As a possible indication Morton Roberts (1960) has found dark marks in 12 out of 32 globular clusters, which he believes are caused by clouds of diffuse matter.

Luminosity Function

Comparison of the luminosity functions for stars in the general field and for members of clusters provides an independent means of testing evolutionary theory. The luminosity function, $\phi(M)$, gives the number of stars per unit volume per magnitude interval as a function of absolute magnitude. The number of stars per cubic parsec of absolute magnitude between M and M + dM is given by

$$dN = \phi(M)\, dM \quad . \qquad (2.23)$$

Evidently, $\phi(M)$ depends on the rate of formation of stars of magnitude M at time t and on the rate of evolution. The luminosity function for main-sequence stars in the solar neighbourhood is obtained by separating the observed stars into main-sequence stars and stars which have left the main sequence. For bright stars, the supergiants and giants are separated from the main-sequence stars by the Hertzsprung gap. The division is somewhat arbitrary for F stars where subgiants merge with the main sequence. The luminosity function for the general field has been studied by many workers. Well known information regarding the shape of the general luminosity function was given by Van Rhijn (1939), though the faint end of the luminosity function is very uncertain. However, Luyten's studies on the distribution of stars with large proper motion have now reached

a limit of $M_v = +20$.

Sandage (1958d) provided the luminosity function for main-sequence stars in the general field which is now adopted.

Knowing the rate of evolution given by the theory and making some assumption on the birth-rate of stars, it is possible to derive from the observed function $\phi(M)$ an "initial" luminosity function, $\psi(M)$ which gives the distribution of luminosities at the time of star formation. Sandage has derived $\psi(M)$ in the following way.

Let $\frac{dN}{dt}(M)$ be the birth-rate of stars at absolute magnitude M. Assuming that the rate of star formation is uniform and independent of time,

$\psi(M)$ will be given by,

$$\psi(M) = \frac{dN}{dt}(M) \cdot T \qquad (2.24)$$

where T is the age of the galaxy.

The life-time of a star on the main sequence is given by

$$\tau = 1{\cdot}10 \times 10^{10} \cdot \frac{M}{L_T} \text{ years.}$$

For faint stars the time spent on the main sequence exceeds the age of the galaxy.

So the observed luminosity function for faint stars is

$$\phi(M) = \frac{dN}{dt}(M) \cdot T \qquad (2.25)$$

When $\tau < T$, stars now on the main sequence formed less than τ years ago. Therefore

$$\phi(M) = \frac{dN}{dt}(M) \cdot \tau(M) \qquad (2.26)$$

Combining (2.24) and (2.26),

$$\psi(M) = \phi(M) \cdot \frac{T}{\tau(M)}$$

$$= \phi(M) \cdot \frac{M_L}{M} \cdot \frac{L_T}{L_L} \qquad (2.27)$$

where M_L and L_L are the mass and luminosity which gives $T = \tau$.

There is a marked difference in the shape of the initial luminosity function and that of the observed general luminosity function. The initial luminosity function is very flat while the other has a steep slope towards brighter magnitudes. This is explained by the fact that there has been evolutionary depletion of brighter stars in the general field.

If the mode of star formation in galactic clusters is the same as in the solar neighbourhood, the observed luminosity function for the galactic clusters should agree with the initial luminosity function $\psi(M)$ (since the stars have formed simultaneously). The evidence given by Sandage indicates that the agreement is fairly good down to $M_v = +6$, but that there are differences for fainter magnitude. For an old cluster, like M67, a theory of the escape of stars from clusters may be

applied, but in younger clusters there has not been sufficient time for the escape of stars. This discrepancy may suggest that the conditions under which low-mass stars in clusters form, differ from the conditions under which average low mass stars are created. Another possible explanation for this discrepancy according to Van den Bergh (1957) is, that some population II stars may have been included in the general luminosity function and that the relative numbers of faint stars may be different in different populations.

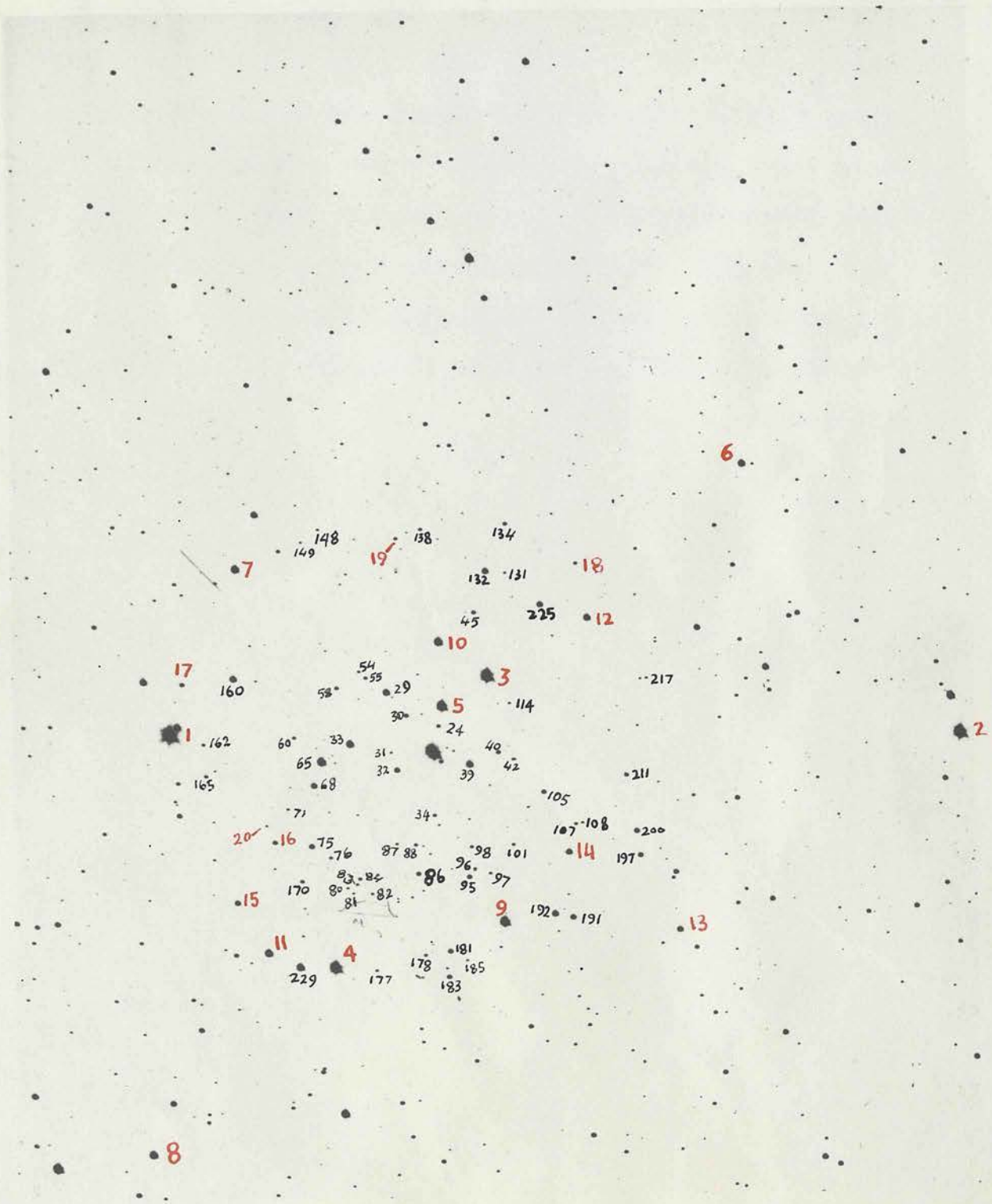

FIG. 5 - NGC 2422
Photoelectric standards are indicated by red figures.

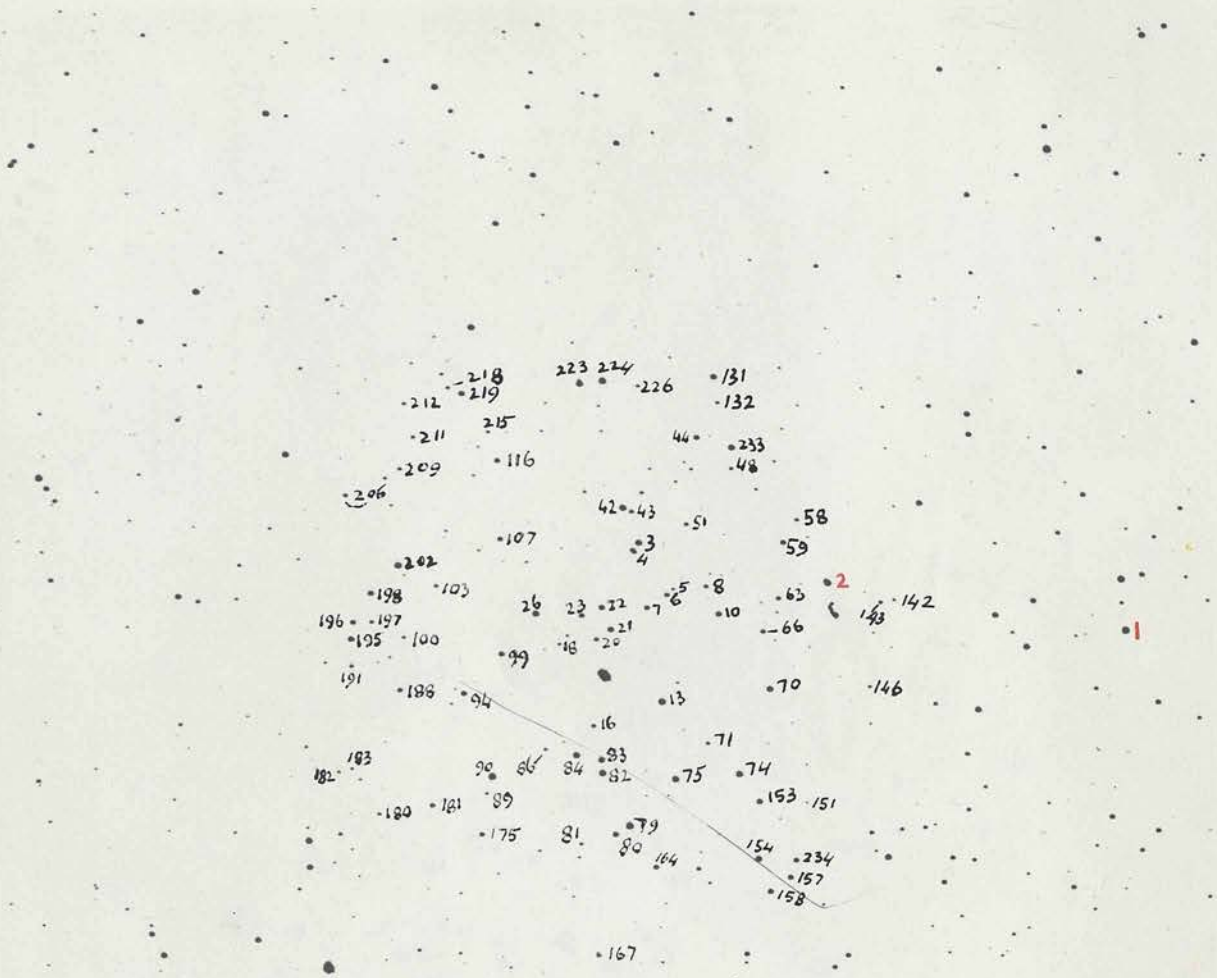

FIG. 6 - NGC 2423
Photoelectric standards are indicated by red figures.

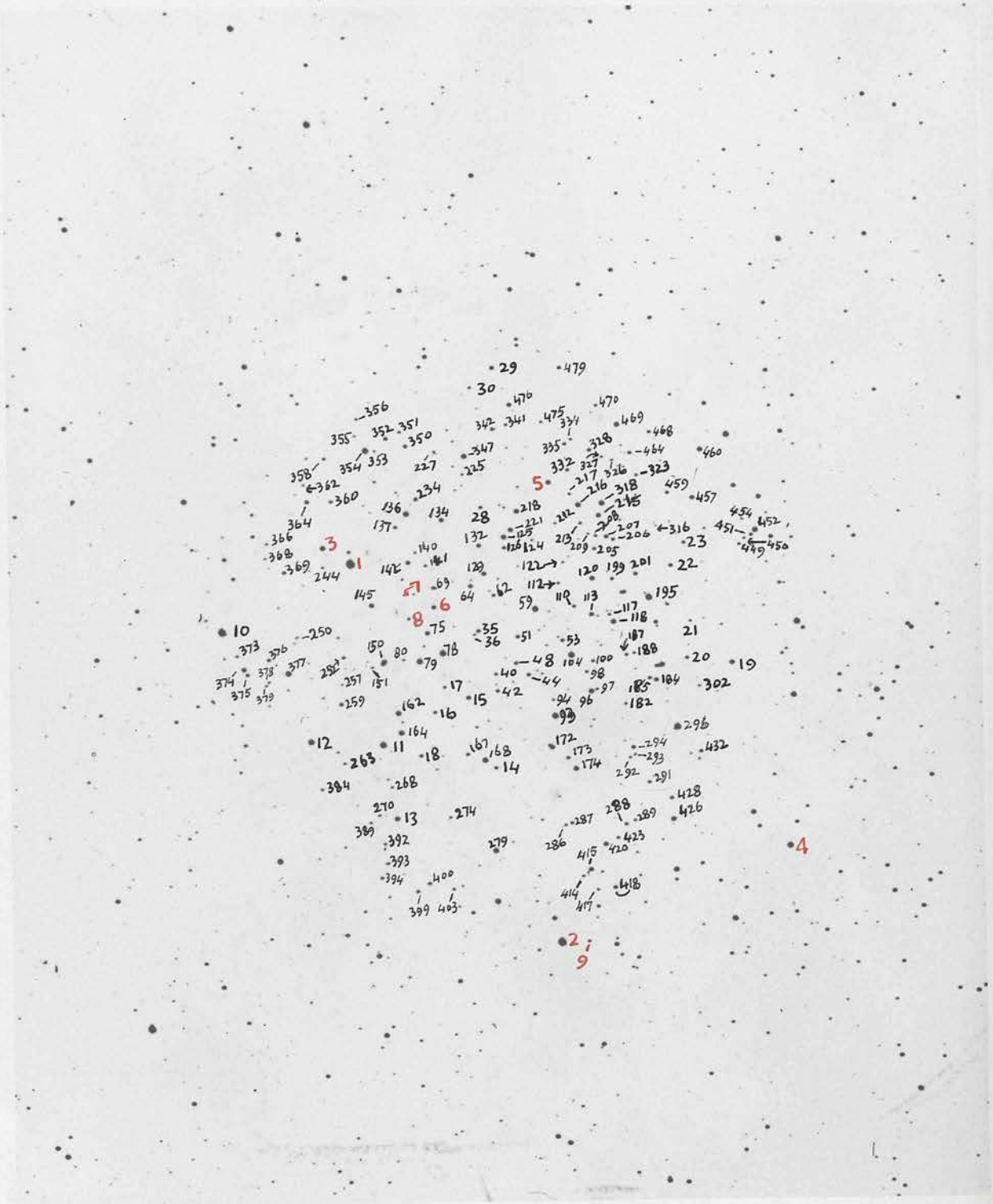

FIG. 7 - NGC 2437
Photoelectric standards are indicated by red figures.

PART II

CHAPTER III

PHOTOMETRY OF SOUTHERN OPEN CLUSTERS

Programme of Work

Programmes of extending three-colour observations on the U, B, V system of Johnson and Morgan to the southern sky have been started by many observatories, including the Royal Observatory, Edinburgh. As a part of this programme three southern galactic clusters NGC 2422, NGC 2423 and NGC 2437 have been investigated by the author. The clusters are situated in the Monoceros region of the Milky Way.

The regions are illustrated in Figures 5, 6 and 7.

The results of other workers and the relevant data are given in Table 2.

Description of Plates

The photographic plates of the clusters were taken with the ADH Schmidt telescope at the Boyden Observatory (South Africa) by Dr. H.E. Butler of the Royal Observatory, (Edinburgh), and Dr. G. Lynga of the Lund Observatory. The plates are detailed in Table 3. The three clusters were taken on the same plate. The positions of the clusters on

(TABLE 2).

Cluster	R.A. 1950	Decl. 1950	Galactic Longi-tude	Galactic Lati-tude	Angular Diameter	Class	Distance in parsec				Colour Excess		No.** of Stars
							Trumpler	Shapley	Collinder	Cuffey≠	Trumpler*	Cuffey≠	
NGC 2422	$7^h34.7^m$	$-14°22'$	$198°.7$	$+4°.4$	30'	II3m	480	720–1150	590		0		50
NGC 2423	$7^h35.3^m$	$-13°46'$	$198°.2$	$+4°.8$	19'	I2m	720	1150–1820	790				60
NGC 2437	$7^h40.1^m$	$-14°44'$	$199°.6$	$+5°.3$	27'	II2r	660	1150–1820	1000	1450		-.2 mag.	150

*Lick Observatory Bulletin 16, No.454, 132, 1932-34.

≠Publications of the Kirkwood Observatory of Indiana University No. 4, 1941.

** Shapley - Star Clusters, p229, 1930

(TABLE 3)

	U						B						V					
	Plate	Filter	Exposure	No NGC 2422	No NGC 2423	No NGC 2437	Plate	Filter	Exposure	No NGC 2422	No NGC 2423	No NGC 2437	Plate	Filter	Exposure	No NGC 2422	No NGC 2423	No NGC 2437
ADH Plates	103ao	UG2	15m	4	4	3	IIao	BG12 +GG18	3m	3	3	4	103aD	GG11	2m	3	3	3
	103ao	UG2	60m	2	2	2	IIao	BG12 +GG18	10m	2	2	1	103aD	GG11	10m	4	4	4
							IIao	BG12 +GG18	30m	2	2	2						
DS	103ao	Chance OXIglass	5m		3		103ao	–	2m	5	6	2	103aE	Wratten No. 25	20m	2	2	2
	103ao	Chance OXIglass	20m	3	1	1												

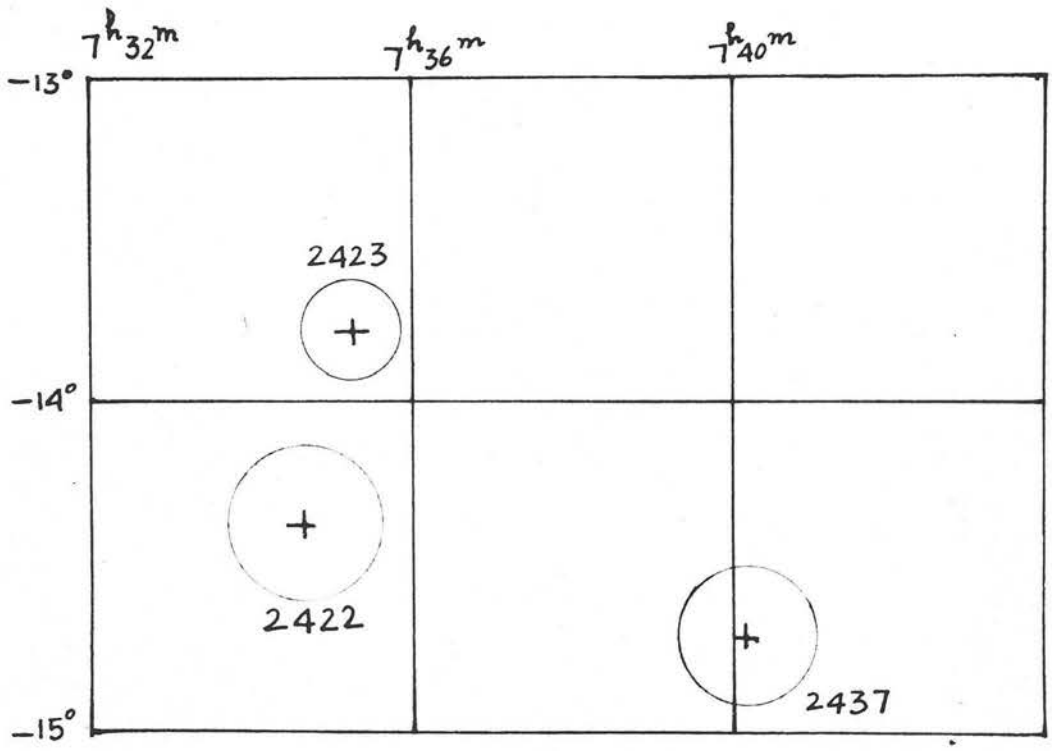

FIG. 8 - Position of the clusters on the plate.

on the plates are schematically shown in Fig. 8.

Photoelectric Standards

As photometric standards, Lynga (1959) determined a photoelectric sequence in the UBV system for cluster NGC 2422. He also measured photoelectrically some stars in NGC 2423 and NGC 2437. These photoelectric observations were made with a photoelectric photometer on the 60-inch Rockefeller reflector of the Boyden Observatory. The filters used were 2mm G11, 1 mm BG12 + 1 mm GG15 and 1 mm UG2. These observations were reduced to standard UBV system through Johnson stars having negative or low positive declinations.

Measurements of the Plates

The plates were measured with the new Becker-type Iris photometer of The Royal Observatory, Edinburgh. Stars were identified from marked charts. The calibration curve was obtained for each run which extended on the average for four hours. Standard stars were measured at the beginning and end of each run for drift control.

Photometer readings for NGC 2422 and NGC 2423, which were measured earlier, were written down and later punched on tape. In between the work on those clusters and that on NGC 2437, the photometer was digitised. The iris readings and the coordinates of stars for NGC 2437 were directly

punched on paper tape, suitable for the Cambridge computer EDSAC II.

Iris Photometer

A plate photometer measures the photographic densities and sizes of star images on photographic plates which result from the photographic action and diffusion of light in the emulsion. Densities and sizes of images are related to apparent magnitudes of the stars. The reduction is based on plotting the photometric readings against the known magnitude of certain standard stars; drawing a smooth curve through these one can interpolate the magnitudes of other stars.

In early plate photometers such as the Stetson, Schilt and Ross photometers, a fixed diaphragm of suitable diameter was used to provide an illuminated spot of constant size on which the star image was placed. The amount of light blocked out of the beam was measured by a thermocouple or a photocell.

Drawbacks in these systems were:

1) a diaphragm of fixed size limits the measuring range,
2) background readings share equally with stellar readings in the reduction of the photometer readings to magnitudes.

To remove these defects H. Siedentopf (1934) replaced the fixed diaphragm by an iris diaphragm which provided a

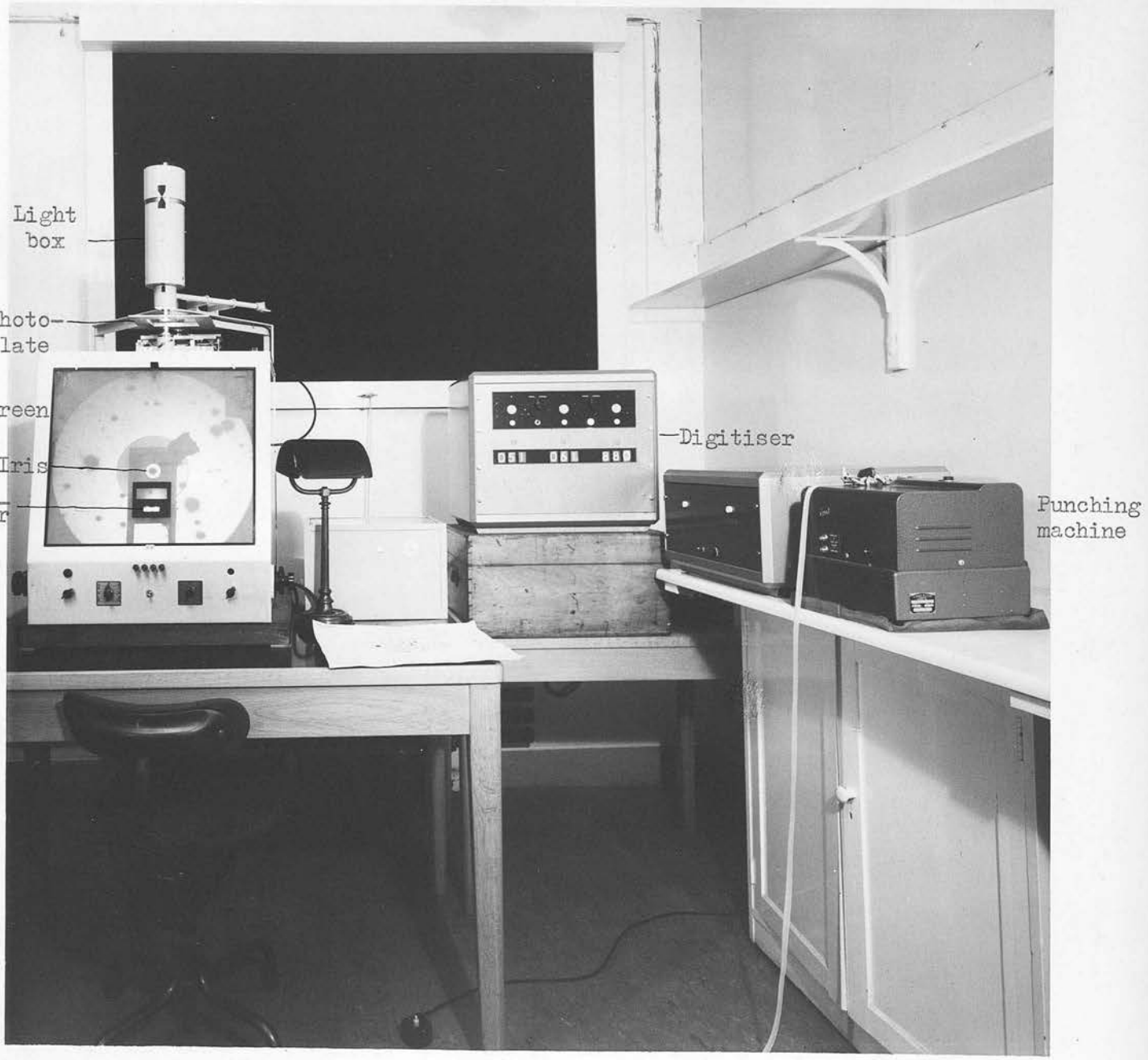

FIG. 9 - The Iris Photometer.

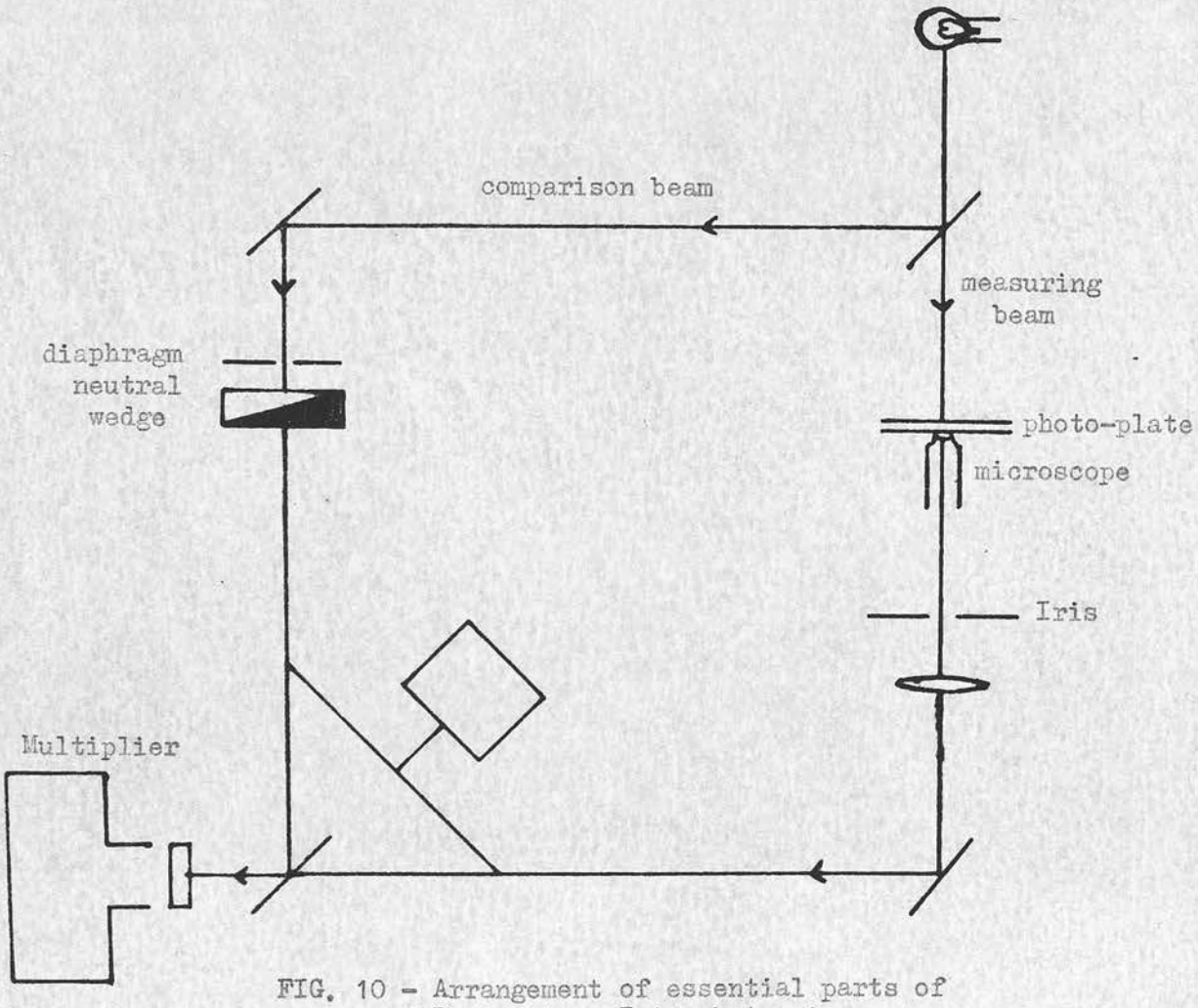

FIG. 10 - Arrangement of essential parts of Becker-type Iris photometer.

spot of varying size. The iris could be adjusted so that the same amount of light passed through and around each stellar image. This arrangement removed most of the drawbacks but there still remained the effect of possible changes in the brightness of the source.

In the "beam comparison method" the photocell, instead of measuring the light which passes through the iris, compares the light coming through the iris image with light direct from the lamp. A change in the brightness of the source will then have no effect on the final measurements.

In practice Eichner (1947), Haffner (1953) and Becker (1956) have all designed iris photometers. The Becker-type photometer is illustrated in Fig. 9. Light from a micro-projection lamp is divided into two beams. The comparison beam is deflected by an adjustable 45^{o} glass plate before it strikes the photographic plate. The aperture of the comparison beam can be regulated by means of a neutral wedge. The measuring beam goes downwards through the plate into the microscope lens. The comparison beam and the measuring beam strike against the photomultiplier alternately. The magnified image of the star is placed on the iris disphragm and the iris is closed till both rays have equal intensity as indicated by the minimum position of the indicator. The optical train is shown in Figure 10.

The principal sources of error in magnitudes derived

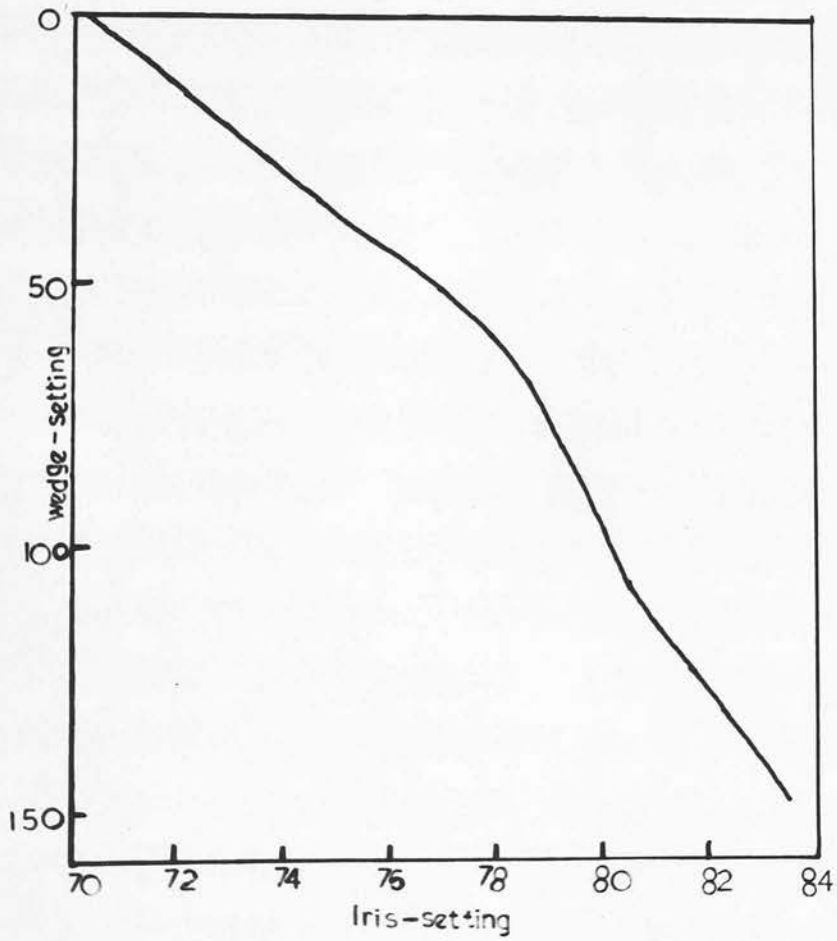

FIG. 11— Wedge-setting against iris-setting.

from photometer readings are the following:

(1) error in centring the star image in the iris diaphragm,

(2) variation in background density,

(3) graininess of the emulsion.

Setting of the Comparison-beam

The intensity of the comparison beam, L_C is balanced by the intensity of light through the photographic image of the star, L_o. L_o is determined by the intensity of illumination of the lamp, the transmission-coefficient of the photographic image and the area of the image, the area being given by the iris-setting. The intensity of illumination is approximately constant withinthe iris and is zero outside. Therefore, for a given star image, the iris settings give a measure of L_o for different apertures of the comparison beam.

The change of iris settings with the wedge-settings (which regulate the aperture of the comparison beam) is shown in Figure 11. The star used for Figure 11 is of the 9th magnitude. To minimise the balancing error, the aperture of the comparison beam, at which the slope in Figure 11 is numerically maximum, has been chosen (Argue, 1960).

Similar curves have been obtained for a number of stars

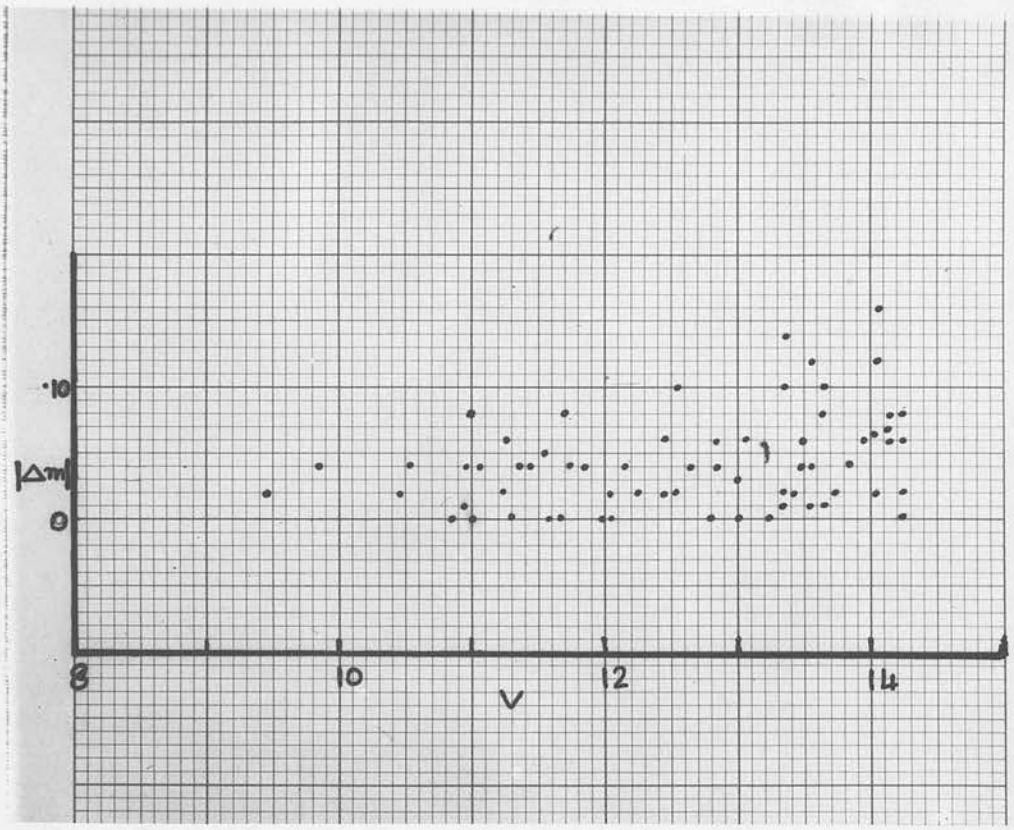

FIG. 12 - Absolute magnitude-difference ($|\Delta m|$) against V-magnitude.

of the same plate. The maximum slope occurs at about the same aperture of the comparison beam. Therefore a single setting of the comparison beam is sufficient over the whole range of measurement.

Magnification

The magnification was changed from plate to plate to make use of the full measuring scale.

Drift

No drift in the zero point has been observed during runs of several hours. The iris-readings for the stars of the standard sequence at the beginning and end of the measuring run do not show any effective drift effect. Very minor differences may be due to centring error.

Consistency of Measurement

To examine the consistency of measurements, a few plates in each colour have been measured twice. The plates have been selected at random and measured at the usual speed.

The differences in magnitudes determined graphically from two measurements of a V plate are plotted for each star in Figure 12. The internal probable error of single measurement is less than $\pm 0^{m}.03$.

Reduction

The iris readings have been reduced to magnitudes by means of the photoelectric magnitude scales obtained for each cluster. For NGC 2423, there are only two sequence stars. Stars of this cluster have been measured with the scale calibrated on the sequences of NGC 2422. To obtain a transfer of scale the two sequence stars of NGC were plotted on the calibration curves for NGC 2422. No systematic effect was found.

It has been necessary to apply colour equations for ADH B- and DS V-plates. Preliminary colour equations have been obtained by smoothing the calibration curves and plotting the mean residuals against (B - V). The colour equations obtained are of the following forms.

For ADH plates:

$$B' - V = 1.2\,(B - V)$$

For DS plates:

$$(B - V') = 1.4\,(B - V) \quad ,$$

where dashes denote the magnitudes in the plate system. The reduction of the data has been carried out with the EDSAC computer at the Cambridge Mathematical Laboratory, using a program developed by Mr. A.N. Argue of the Cambridge Observatories.

The iris-readings are related to magnitudes by the equation

$$m(\theta) = a_0 + a_1\theta + a_2\theta^2$$

where m denotes the magnitude in the plate system,

θ iris-readings

and a_0, a_1 and a_2 are constants.

The constants are estimated by minimising the sum of the squares of the residuals, i.e.

$$\sum_{i=1}^{n} \left(m_i - a_0 - a_1 \theta_i - a_2 \theta_i^2 \right)^2 = \text{minimum},$$

where n is the number of calibration stars. The estimate of the variance of the magnitude determination is given by

$$\sigma^2 = \frac{S^2}{n-3}$$

where $S^2 = \sum m^2 - a_0 \sum m - a_1 \sum m\theta - a_2 \sum m\theta^2$

For illustration, values of σ^2 are shown for some calibration curves in Table 4.

TABLE 4

Variance for degree 0, 1, 2 (unit: square (magnitude)^2)

	0	1	2
ADH 4285(B)	.347	.044	.006
ADH 4322(B)	.371	.013	.004
ADH 4342(V)	.386	.013	.008
ADH 4350(V)	.418	.020	.003
ADH 4348(U)	.297	.058	.006
ADH 4335(U)	.296	.030	.004
DS 107(B)	.438	.092	.006
DS 84(V)	.445	.039	.004
DS 134(U)	.330	.089	.007

TABLE 5

Star No.	Magnitude (graphical)	Magnitude (Computer)	(Computer minus graphical)
4	12.37	12.48	- .11
10	12.26	12.32	- .04
13	11.28	11.33	- .05
16	13.36	13.40	- .04
21	12.00	12.13	- .13
22	12.17	12.29	- .12
26	11.65	11.76	- .11
41	14.01	13.97	.04
44	12.53	12.61	- .08
63	13.06	13.16	- .10
74	11.40	11.52	- .12
79	10.78	10.88	- .10
80	12.24	12.25	- .01
84	11.50	11.56	- .06
99	12.41	12.53	- .12
116	12.74	12.81	- .07
143	13.43	13.51	- .08
175	12.83	12.89	- .06
198	12.16	12.24	- .08
209	13.68	13.75	- .07

In averaging, the criterion of rejection has been prescribed in the program as

$$|\bar{m} - m_i| > \quad 0.4 \ .$$

In Table 5 results obtained from the computer are compared with the graphically derived magnitude of some stars of NGC 2423.

The final transformation equations from the plate system to the standard system have been obtained by a least square solution.

ADH and DS plates have been reduced separately because of different colour equations. Down to 14^m the magnitudes obtained from two sets of plates agree well. Beyond 14^m, where the magnitudes are extrapolated, large differences appear. This indicates that the magnitudes of the stars fainter than the lowest sequence star are quite uncertain.

The final magnitude for each star is obtained by taking the weighted mean of the magnitudes determined on ADH and DS plates, the weighted mean being

$$\frac{n_1 m_1 + n_2 m_2}{n_1 + n_2}$$

where n_1 and n_2 are number of determinations and m_1 and m_2, the magnitudes.

Error

The standard error of a single measurement is shown in the following table.

TABLE 6

	V		B		U	
	$<12^m$	$>12^m$	$<12^m$	$>12^m$	$<12^m$	$>12^m$
Standard error	·046	·054	·052	·056	·053	·058

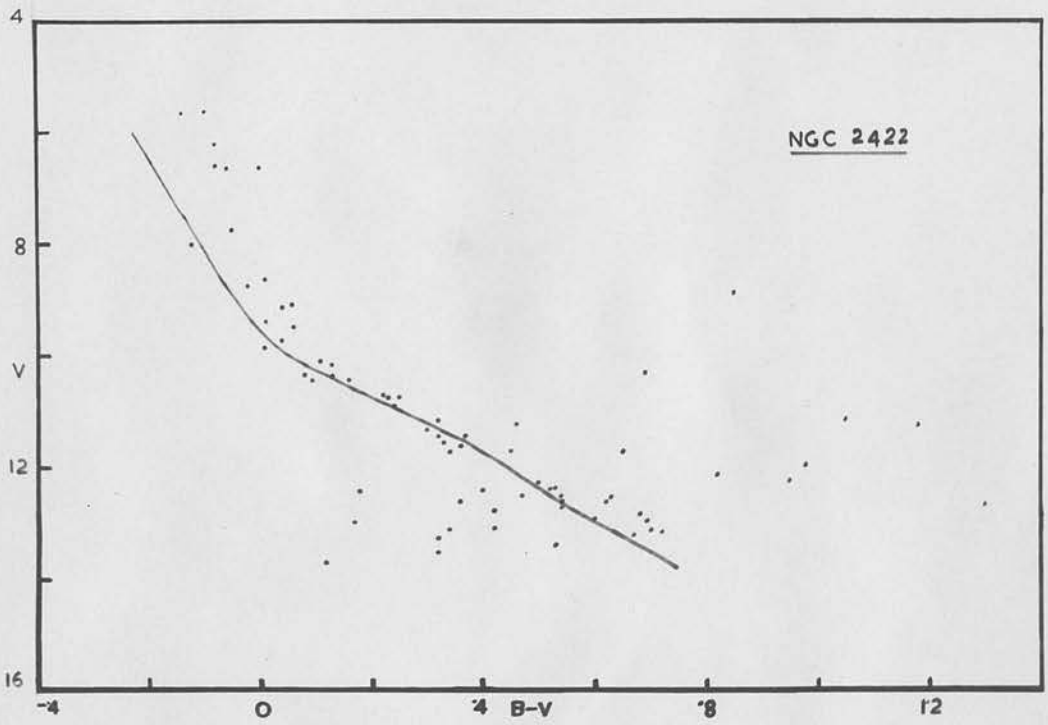

FIG. 13 - The (V, B-V) - diagram of NGC 2422. The solid line denotes the "age-zero sequence" of Johnson and Iriarte (1958).

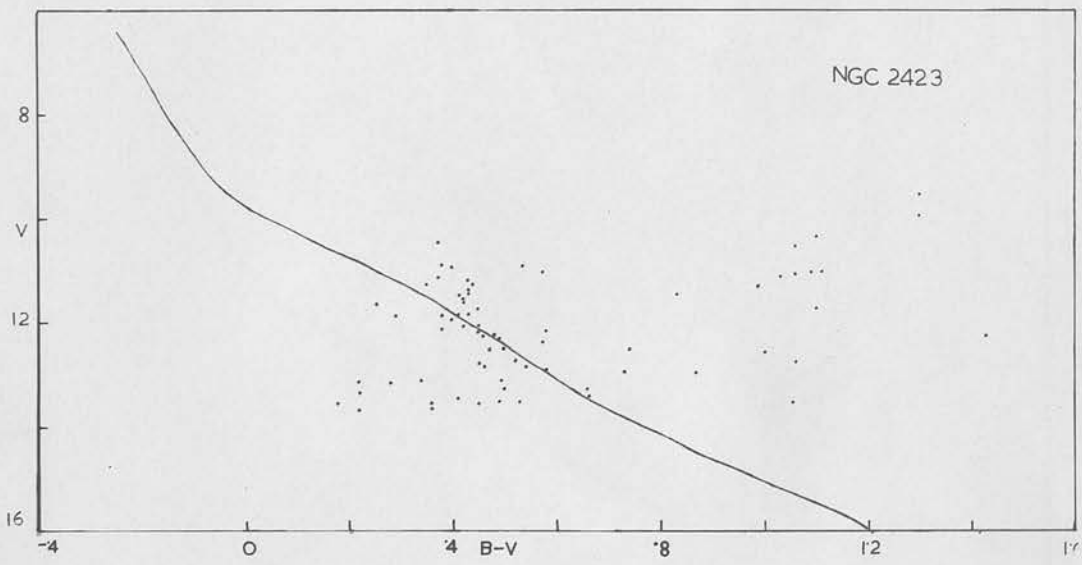

FIG. 14 - The (V, B-V) - diagram of NGC 2423. The solid line denotes the "age-zero sequence" of Johnson and Iriarte (1958).

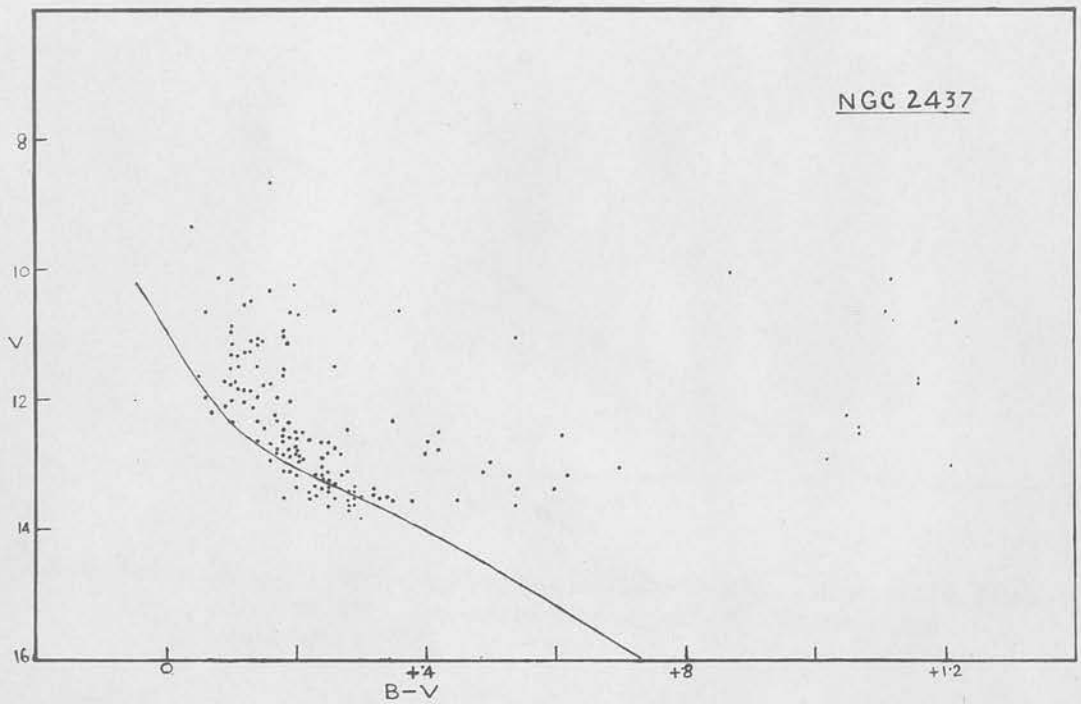

FIG. 15 - The (V, B-V) - diagram of NGC 2437. The solid line denotes the "age-zero sequence" of Johnson and Iriarte (1958).

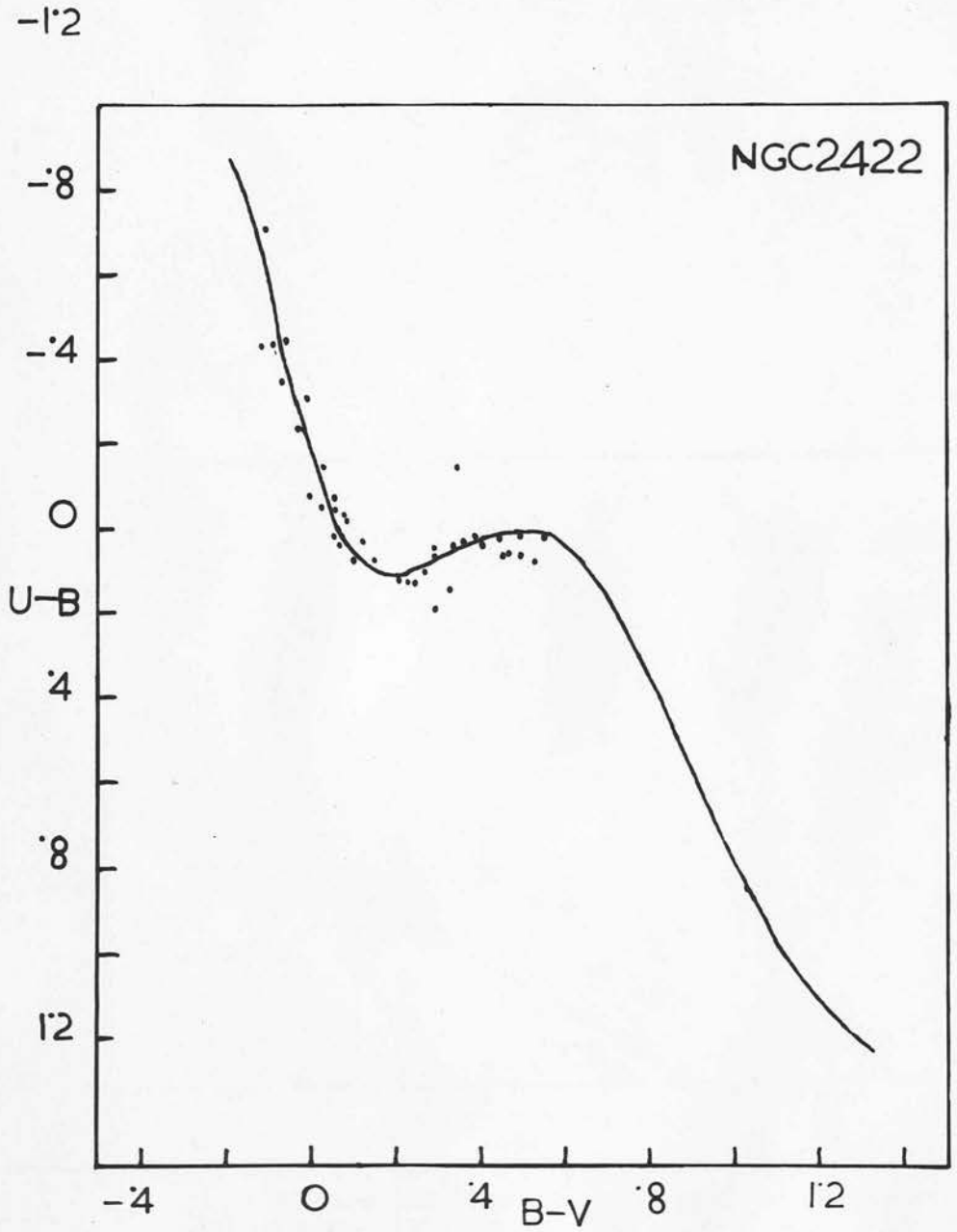

FIG. 16 - The (U-B, B-V) diagram for the stars of NGC 2422 which lie near the cluster main sequence. The solid line represents the standard (U-B, B-V) - relation for main sequence stars, shifted for a reddening of $E_{B-V} = 0^m.06$; $E_{U-B}/E_{B-V} = .72$.

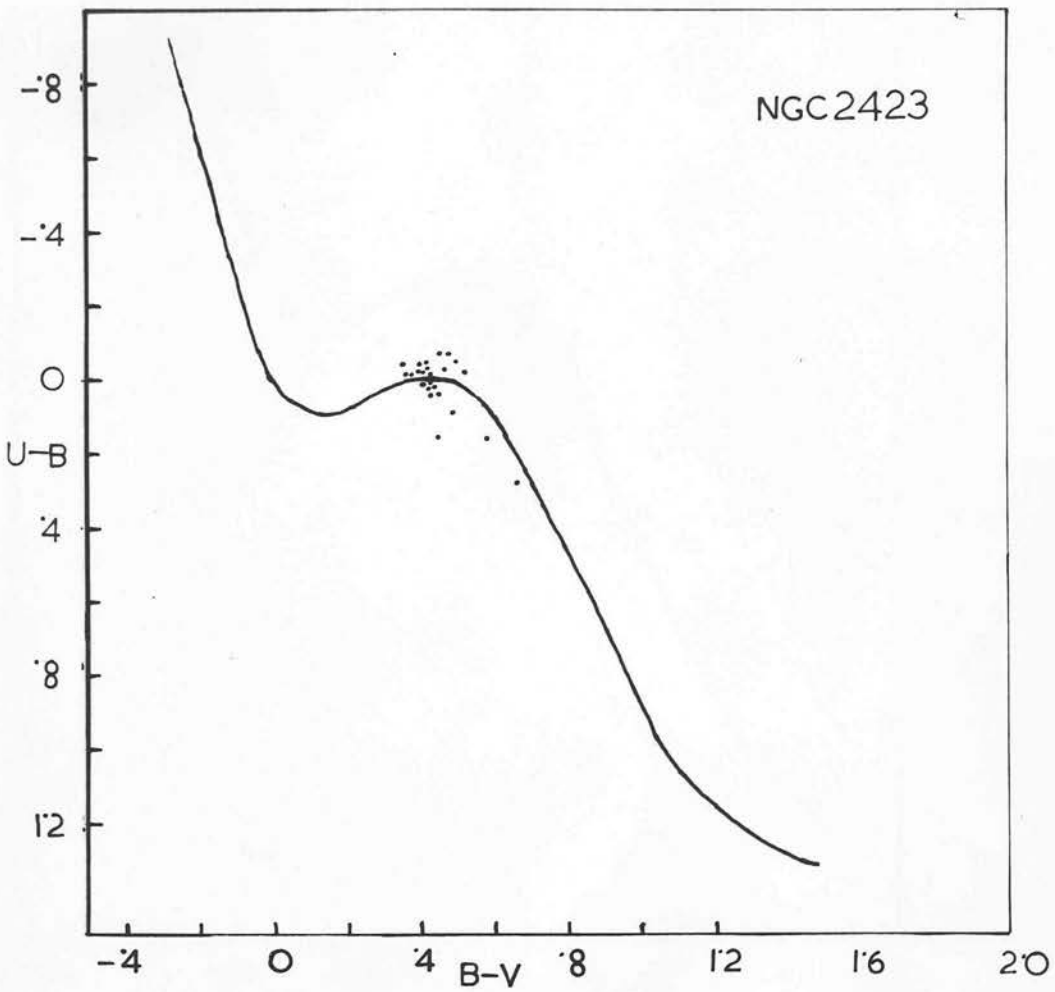

FIG. 17 - The (U-B, B-V) diagram for the stars of NGC 2423 which lie near the cluster main sequence. The solid line represents the standard (U-B, B-V) - relation for main-sequence stars.

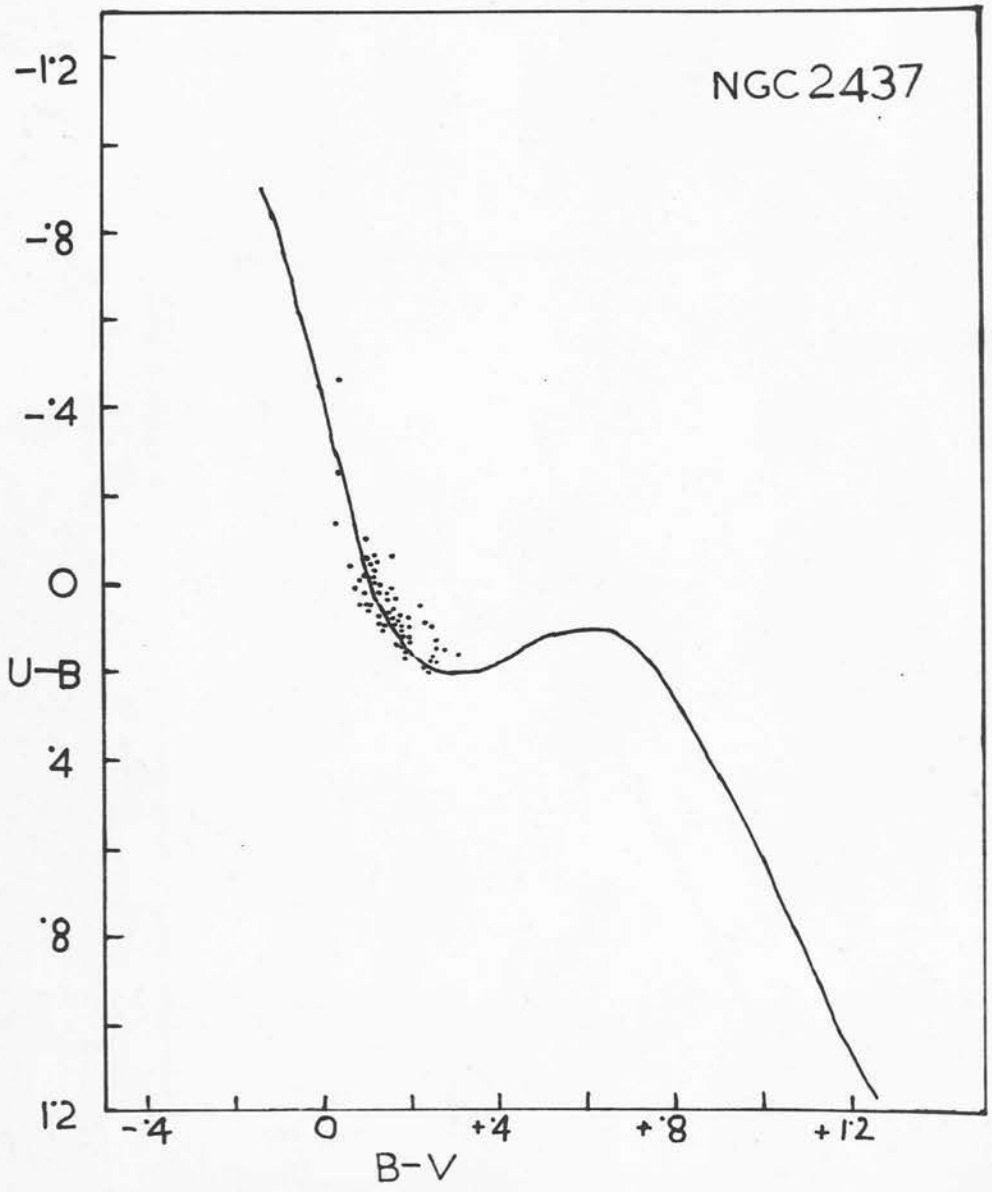

FIG. 18 - The (U-B, B-V) diagram for the stars of NGC 2437 which lie near the cluster main sequence. The solid line represents the standard (U-B, B-V) - relation for main sequence stars, shifted for a reddening of $E_{B-V} = 0^m.16$; $E_{U-B}/E_{B-V} = .72$.

Photometric Results

The observed magnitudes and colours for the three clusters are listed in Tables 7, 8 and 9. The stars fainter than 14th magnitude have been excluded. The first column gives the number of the star, the second, third and fourth, the V magnitude, and the colour indices (B-V) and (U-B). The stars used for calibration are marked with an asterisk.

The V versus (B-V) diagrams for three clusters are shown in Figures 13, 14 and 15. Figures 16, 17 and 18 represent (U-B), (B-V) diagrams for the stars which lie close to the main sequences of the clusters. The effects of reddening on clusters have been determined both by the shift of the main-sequences in the (U-B), (B-V) diagrams along the reddening line and by the "Q" method as modified by Johnson (1958).

The apparent distance moduli have been determined by fitting the cluster main sequences in the V versus (B-V) diagram to the standard initial main sequence (Johnson and Iriarte, 1958). For NGC 2422 and NGC 2437, only stars about 3 magnitudes fainter than the brightest ones have been used to minimise evolutionary effects. For NGC 2423, the main sequence stars are fewer, and stars in the vicinity of V = 12, B-V = .4 have been used.

The results are summarised in Table 10.

The probable error of the distance moduli due to the uncertainty in the fitting is $\pm$ $0^{m}.2$ approximately.

TABLE 7

NGC 2422

Star No.	V	B-V	U-B
1 *	5.66	-.10	-.72
2 *	6.51	0.00	-.31
3 *	6.68	-.06	-.35
4 *	7.01	-.08	-.44
5 *	7.76	-.05	-.44
6 *	7.79	1.68	1.82
7 *	7.80	1.21	1.11
8 *	7.91	1.03	0.77
9 *	8.02	-.12	-.44
10 *	8.76	-.02	-.24
11 *	9.11	.06	-.08
12 *	9.76	.04	-.06
13 *	10.47	.16	.07
14 *	10.48	.09	-.04
15 *	10.72	.22	.11
16 *	11.53	.45	.01
17 *	11.64	.36	-.25
18 *	12.40	.52	.13
19 *	12.54	.47	.05
20 *	13.68	.39	
24	12.06	.40	.02
29	8.91	.85	.36
30	11.44	.34	.04
31	13.72	.31	
32	10.77	.23	.08
33	9.41	.01	-.09
34	12.38	.53	.01
39	9.57	.06	-.05
40	11.74	.35	.14
42	12.62	.62	
45	11.68	.43	.01
54	12.95	.60	
55	12.74	.15	.23
58	11.27	1.17	1.03
60	12.62	.38	.19
65	8.64	.02	-.24
68	10.40	.13	.08
71	13.53	.32	
75	10.89	.23	.13
76	12.71	.54	.08
80	13.47	.51	
81	13.53	.64	.29
82	13.28	.31	.42
83	13.01	.69	.39
84	12.52	.50	.06
86	11.58	.33	.03

TABLE 7 (Contd.)

NGC 2422

Star No.	V	B-V	U-B
87	13.67	.12	.03
88	12.39	.56	.01
95	11.24	.46	.06
96	12.15	.82	
97	12.84	.68	
98	12.82	.39	.25
101	13.00	.27	
105	11.45	.30	.19
107	12.53	.62	.17
108	13.17	.61	.29
114	13.42	.53	
131	13.15	.70	
132	10.09	.12	.02
134	11.75	.65	.19
138	11.92	.98	.56
148	13.12	.54	.40
149	12.69	1.30	
160	9.88	.01	-.05
162	12.61	.52	
165	12.28	.50	0
170	12.40	.19	.16
177	13.11	.46	.16
178	12.27	.95	.54
181	11.16	.32	.06
183	11.41	.37	.03
185	13.45	.58	.43
191	10.72	.25	.12
192	10.11	.11	.06
197	11.10	.28	.10
200	10.35	.69	.29
211	11.19	1.05	.66
217	13.22	.67	
225	10.37	.08	.04
229	9.16	.04	-.15

TABLE 8

NGC2423

Star No.	V	B-V	U-B
1 *	9.42	1.42	1.41
2 *	10.83	0.34	0.12
3	10.63	1.11	.63
4	11.49	.83	-.04
5	13.55	.53	
6	12.42	.50	.05
7	11.73	1.10	.86
8	12.54	.74	.33
10	11.85	.41	-.04
13	10.89	.38	-.01
16	12.75	.52	-.02
18	13.57	.45	
20	12.79	.45	.02
21	11.64	.43	.04
22	11.91	.29	.02
23	12.27	.48	-.07
26	11.23	.44	.02
42	11.20	.43	.01
43	12.84	.46	-.06
44	12.10	.43	.02
48	13.59	.17	
51	13.15	.49	-.01
58	13.19	.42	
59	12.05	.43	-.10
63	12.57	.47	-.03
66	12.40	.57	0
70	11.31	.41	-.02
71	12.58	1.00	
74	11.12	.35	-.04
75	10.88	.53	-.03
79	10.45	.37	.62
80	11.04	1.03	.62
81	13.30	.50	
82	9.95	1.30	1.04
83	11.34	.43	-.02
84	11.13	.37	-.01
86	12.78	1.06	
89	13.51	.49	
90	9.58	1.30	1.06
94	11.98	.40	-.02
99	12.04	.42	.01
100	13.68	.22	
103	12.98	.58	
107	12.50	,.32	.09
116	12.26	.46	.07
131	11.05	1.06	.55
132	13.48	.41	
142	13.59	.36	
143	13.19	.28	

TABLE 8 (Contd.)

NGC 2423

Star No.	V	B-V	U-B
146	13.27	.66	
151	13.51	1.07	
153	11.65	.25	.01
154	11.04	.57	-.07
157	11.04	1.09	.59
158	11.59	.42	-.03
164	11.86	.56	-.09
167	12.42	.43	.05
175	12.19	.58	-.07
180	13.38	.22	
181	12.17	.45	.04
182	13.61	.36	
183	12.97	.87	
188	12.38	.49	.09
191	12.83	.54	
195	11.61	.42	-.05
196	12.17	.38	.07
197	13.11	.34	
198	11.73	.45	.16
202	10.38	1.10	.66
206	13.15	.22	
209	13.59	.09	
211	12.28	1.43	
212	13.65	.12	
215	13.41	.66	
218	12.98	.73	
219	11.31	.99	.44
223	10.52	1.06	.57
224	10.98	.40	-.01
226	13.54	.36	
233	11.38	.43	-.02
234	11.86	.36	-.01

TABLE 9

NGC 2437

Star No.	V	B-V	U-B
1*	8.68	.16	-.07
2*	9.39	.03	-.14
3*	10.19	1.12	0.79
4*	10.95	.10	-.02
5*	11.05	.54	.03
6*	11.96	.16	.01
7*	12.90	1.36	-
8*	13.23	.24	.20
9*	13.35	.20	.14
10	9.38	.04	-.47
11	10.34	.16	.08
12	10.67	.26	.13
13	11.56	.18	.06
14	12.79	.25	.09
15	12.05	.10	-.04
16	12.85	.08	.14
17	13.25	.25	.09
18	12.80	.20	.08
19	11.70	.09	-.05
20	12.70	.17	.14
21	13.03	.70	
22	12.30	.10	.06
23	11.79	1.16	.71
28	12.60	.21	.16
29	10.81	1.22	.71
30	13.04	.24	.16
35	12.30	.14	.11
36	13.49	.34	.11
40	12.24	1.05	.51
42	12.64	.16	.06
44	12.63	.14	.06
48	12.51	.20	.12
51	12.38	.18	.13
53	12.33	.31	.07
59	10.53	.12	-.03
62	12.65	.41	.01
64	12.01	.18	.07
69	12.35	.20	.10
70	11.81	.15	.10
78	10.42	.13	-.05
79	10.69	.23	.05
80	13.61	.25	
93	10.69	.06	.04
94	13.64	.30	
96	11.48	.14	.06
97	13.41	.24	.10
98	13.15	.23	-
100	12.94	.17	.09
104	10.50	.13	0

TABLE 9 (Contd.)

Star No.	V	B-V	U-B
110	12.79	.21	.09
112	13.04	.53	-.07
113	11.85	.13	.09
117	13.16	.20	.09
118	11.19	.10	-.05
120	11.53	.11	.05
122	13.58	.33	
124	13.37	.50	
125	11.34	.13	.10
126	12.51	.18	.11
129	11.72	.20	.03
132	12.00	.18	.10
134	11.77	.16	.08
136	10.68	.19	.17
137	12.56	.24	.09
140	13.47	.28	
141	12.41	1.07	
142	11.98	.14	.10
145	11.44	.31	.10
150	10.11	.87	.40
151	13.47	.32	
162	11.27	.13	0
164	11.26	.12	-.06
167	12.87	.19	.08
168	11.07	.15	.02
172	11.72	.11	-.05
173	12.81	.20	.08
174	10.67	1.11	.63
182	13.54	.19	.08
184	12.21	.08	.01
185	12.77	.19	.14
187	12.89	.24	.09
188	12.54	1.07	
195	10.21	.08	.01
199	11.73	1.16	.76
201	12.24	.17	.10
205	12.61	.24	.08
206	12.48	.28	.12
207	12.10	.09	-.01
208	12.82	.27	.12
209	13.52	.35	
212	13.37	.28	
213	12.05	.10	
215	11.51	.10	0
216	11.08	.14	.07
217	13.19	.24	.10
218	11.32	.10	.05
221	11.50	.26	.07
225	13.35	.25	.17
227	12.98	.51	.04
234	12.02	.30	.16
244	13.31	.29	
250	13.24	.66	

TABLE 9 (Contd.)

Star No.	V	B-V	U-B
252	12.89	.20	.08
257	13.52	.85	
259	12.43	.17	.08
263	13.44	.22	
268	12.94	1.02	
270	13.52	.22	
274	13.60	.30	
279	11.16	.19	.12
286	13.27	.45	-.07
287	12.77	.42	.02
288	12.79	.17	.10
289	13.18	.53	-.08
291	13.12	.18	.10
292	13.51	.29	
293	13.31	.60	
294	12.43	.18	.08
296	10.21	.10	-.02
302	13.61	.53	
316	13.56	.44	
318	10.88	.10	-.09
323	13.08	.24	
326	13.45	.29	
327	13.39	.24	
328	12.13	.09	-.01
332	12.58	.18	.12
334	13.10	.25	.09
335	12.49	.26	.11
341	12.54	.61	-.04
342	12.31	.35	.21
347	11.03	.17	.03
350	12.01	.19	.15
351	12.93	.20	.08
352	12.00	.17	.11
353	13.61	.28	
354	10.27	.19	.12
355	13.61	.29	
356	13.13	.25	.13
358	12.86	.18	.14
360	12.57	.19	.14
362	13.51	.34	
364	11.87	.13	.08
366	13.39	.32	.10
368	13.56	.28	
369	12.37	.19	.12
373	13.30	.23	.09
374	11.64	.18	.18
375	12.59	.22	.17
376	11.61	1.32	.77
377	10.67	.32	.11
378	13.23	.69	
379	13.37	.54	
384	13.30	.26	

TABLE 9 (Contd)

Star No.	V	B-V	U-B
389	13.50	.33	
392	13.45	.23	
393	13.21	.27	.05
394	12.68	.65	.02
399	12.93	.20	.10
400	12.76	.26	.12
403	13.25	.26	.15
414	13.43	.25	
415	12.01	.12	.01
417	13.19	.62	
418	12.53	.18	.09
420	11.86	.12	.01
423	13.19	.20	.10
426	11.62	.05	-.25
428	12.75	.20	.09
432	12.77	.17	.06
449	13.11	.19	.10
450	13.09	.49	
451	12.50	.42	0
452	10.96	.18	.10
454	13.61	.28	
457	11.75	.10	-.07
459	12.66	.25	.11
460	11.28	.12	-.02
464	12.50	.21	.10
468	12.65	.18	.03
469	11.19	.14	.06
470	12.84	.40	.08
475	13.16	.28	.15
476	11.84	.11	.01
479	12.32	.26	.13

TABLE 10

Cluster	Reddening	Apparent Distance Modulus	True Modulus	Distance in Parsecs
NGC 2422	.06	8.6	8.42	480
NGC 2423	0	8.3	8.3	450
NGC 2437	.16	11.30	10.82	1450

FIG. 19 - (M_V, B-V) - diagram for NGC 2422, superimposed on Sandage's diagram of galactic clusters. Ages correspond to the brighter termination points of main sequences.

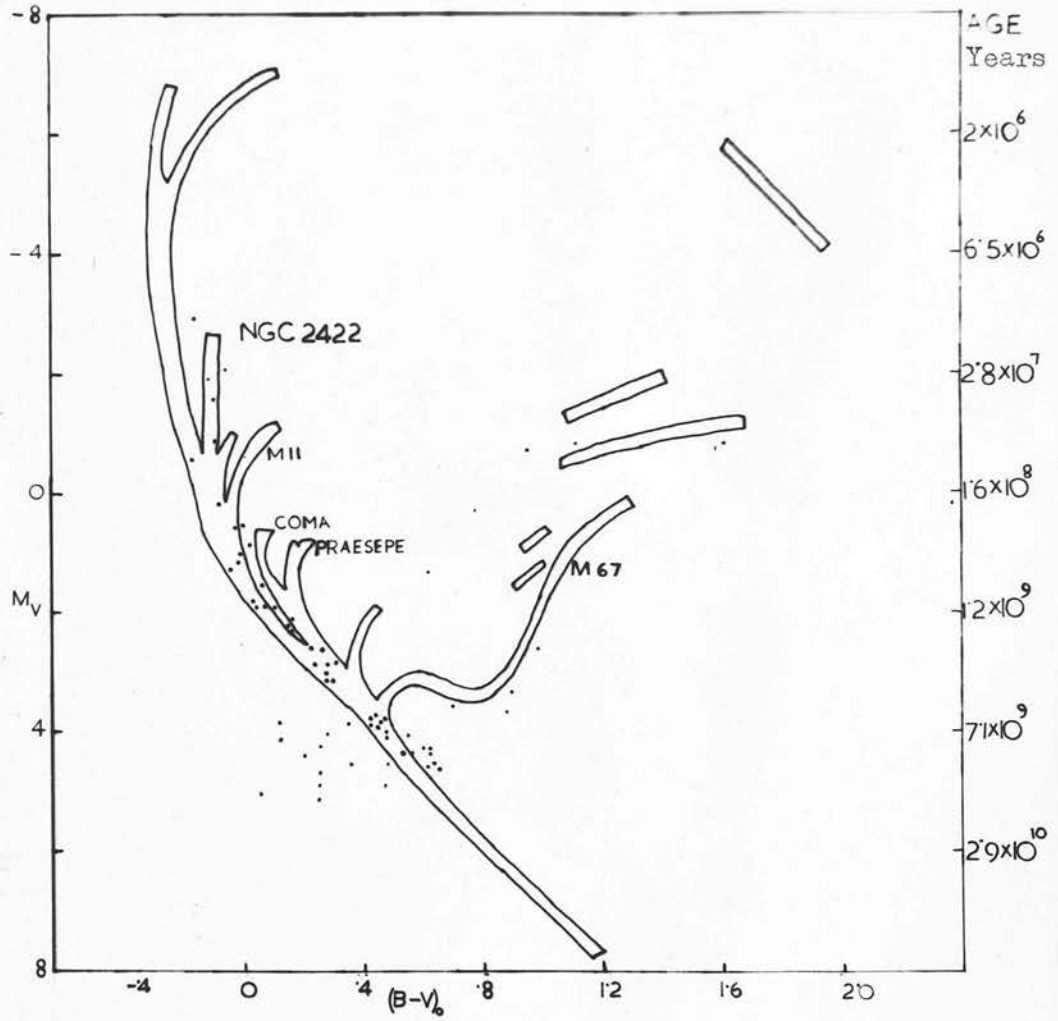

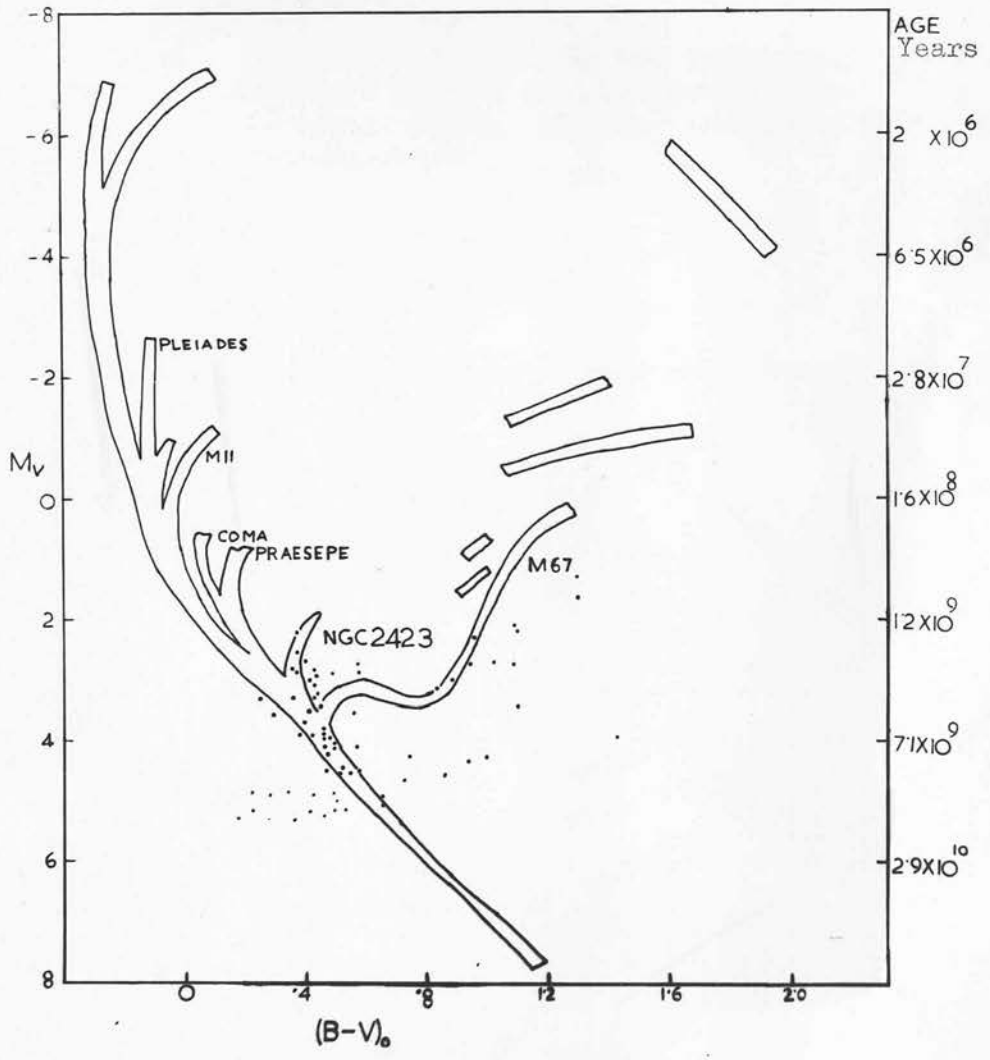

FIG. 20 – (M_V, B-V) – diagram for NGC 2423, superimposed on Sandage's diagram of galactic clusters. Ages correspond to the brighter termination points of main sequences.

FIG. 21 – (M_V, B–V) – diagram for NGC 2437, superimposed on Sandage's diagram of galactic clusters. Ages correspond to the brighter termination points of main sequences.

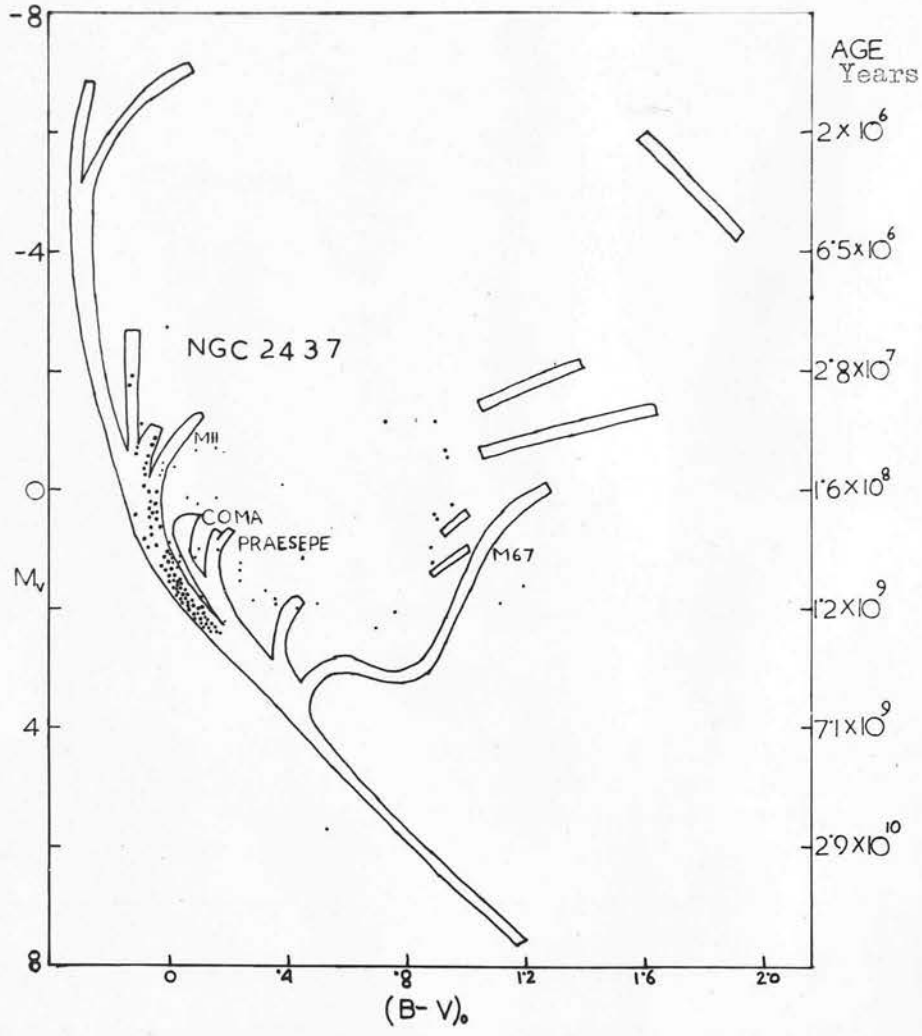

DISCUSSION

The evolutionary features of the clusters are revealed when their resulting colour-absolute magnitude diagrams are superposed on the schematic colour-magnitude diagrams for galactic clusters (Figs. 19, 20, 21).

NGC 2422

The appearance of the colour-magnitude diagram for NGC 2422 is strikingly similar to that of the Pleiades. The cluster shows a well defined main sequence. The turn off point at the bright end of the main sequence is nearly the same as that of the Pleiades, which indicates that the cluster is nearly as old as the Pleiades.

If the photometry could have been carried to the fainter stars of the main sequence, it would have been interesting to see whether there is any break, as in the Pleiades, at the lower end of the main sequence.

NGC 2423

The cluster shows a small part of the main sequence. Absence of bright stars indicates that this is a relatively old cluster.

The characteristic curve at the upper end is similar to NGC 752. However, the giant sequence of this cluster is not very clearly marked. Stars which appear to form a giant sequence, may actually not be members of these clusters.

An important problem in the study of H-R diagrams of clusters of different ages, is to determine exactly the place where the Hertzsprung gap first becomes apparent. A critical study of this cluster may be useful in this respect.

NGC 2437

The cluster contains a few luminous B type stars with absolute magnitudes as high as $M_v = -1.8$. The main sequence of this cluster has the shape characteristic for young clusters like the Pleiades. There is an indication of a giant sequence around $M_v = -1$, $B-V = +.9$, leaving a Hertzsprung gap between the giant sequence and main sequence. The width of the observed gap is about $1.^m0$ in B-V. The width of the Hertzsprung gap in M41 is about $1.^m0$ in B-V.

A group of five giants of lower luminosities appear around $M_v = +1$, $B-V = .9$. This has also been mentioned by Cuffey (1941). These giants are distributed around the centre of the cluster and it may be that they are cluster members. Their position is not clear. A possible explanation is that these stars have suffered considerable mass-loss and have reached the position appropriate to lower-mass stars.

ACKNOWLEDGEMENT

The work has been carried out under the supervision of Professor H.A. Brück and Dr. M.J. Smyth to whom I am gratefully indebted for their valuable guidance.

I would like to express my thanks to Dr. H.E. Butler and Dr. G. Lynga for making the plates available to me.

For the reduction work, I am grateful to Mr. A.N. Argue of the Cambridge Observatories for his help in the processing of the data on EDSACII and for the use of his programme.

The opportunity to work at the Royal Observatory has been made possible by generous grants of the International Astronomical Union and the Cormack Bequest of The Royal Society of Edinburgh.

REFERENCES

(1) Argue, A.N.: Vistas in Astronomy, Vol. 3, p. 184, Pergamon Press, 1960.

(2) Argue, A.N.: Monthly Notices Roy. Astronom. Soc. 122, 197, 1961.

(3) Arp, H.C.: Astronom. Journ. 64, 441, 1959.

(4) Becker, W.: Astrophys. Journ. 107, 278, 1948.

(5) Becker, W. & Biber, C.: Z. Astrophys. 41, 52, 1956.

(6) Becker, W. & Steinlein, U.: Z. Astrophys. 39, 188, 1956.

(7) Bergh, S. Van Den: Astrophys. Journ. 125, 445, 1957.

(8) Biermann, L.: Gas Dynamics of Cosmic Clouds, I.A.U. Symposium No. 2, Chapter 39, 1955.

(9) Biermann, L.: Z. Astrophysics 25, 161, 1948.

(10) Biermann, L.: Astronom. Nachr. 264, 361, 1938.

(11) Blanco, V.M.: Astrophys. Journ. 123, 64, 1955.

(12) Bonsack, W.K., J.L. Greenstein, J.S. Mathis, W.G. Melbourne, G. Neugebauer, R.L. Newburn, K.H. Olsen, W.G. Tifft, H.D. Wahlquist & G. Wallerstein: Astrophys. Journ. 125, 139, 1957.

(13) Burbidge, E.M. & Sandage, A.R.: Astrophys. Journ. 128 174, 1958.

(14) Cox, A.N.: Lecture Notes, International Summer Course in Science, NUFIC (Netherlands. University Foundation for International Co-operation), IV.4, The Hague, 1960.

(15) Cox, A.N.: Astrophys. Journ. 119, 188, 1954.

(16) Cuffey, J.: Publications of the Kirkwood Observatory of Indiana University, No. 4, p. 55, 1941.

(17) Demarque, P.: Astrophys, Journ. 132, 366, 1960.

(18) Eggen, O.J.: Astrophys. Journ. 111, 65, 1950.

(19) Eichner, L.C., Hett, J.H., Schilt, J., Schwarzschild, M. & Sterling, H.T.: Astronom. Journ. 53, 25, 1947.

REFERENCES (Contd.)

(20) Fessenkov, V.G.: Trans. I.A.U. 8, 702, 1952.

(21) Fowler, W.A.: "Modeles d'Etoiles et Evolution Stellaire", Mem. Soc. Roy. Sci., Liege, 5e Serie, T.III, 1960.

(22) Greaves, W.H.M.: Trans. I.A.U. 8, 355, 1952.

(23) Greenstein, J.L.: Astrophys. Journ. 117, 269, 1953.

(24) Haffner, H.: Veröff. Sternwarte Göttingen, No. 106, 1953.

(25) Harrison, M.H.: Astrophys. Journ. 100, 343, 1944.

(26) Hasselgrove, C.B. & Hoyle, F.: Monthly Notices Roy. Astronom. Society, 116, 515, 1956.

(27) Henyey, L.G.: Ledevier, R. & Levee, R.D.: Publ. Astronom. Soc. Pacific, 67, 154, 1955.

(28) Hiltner, W.A. & Johnson, H.L.: Astrophys. Journ. 124, 367, 1956.

(29) Hoerner, S. Von: Z. Astrophysics, 42, 273, 1957.

(30) Hoyle, F. & Haselgrove, C.E.: Monthly Notices Roy. Astronom. Soc. 119, 112, 1959.

(31) Hoyle, F.: Astrophys. Journ. 124, 482, 1956.

(32) Hoyle, F. & Schwarzschild, M.: Astrophys. Journ. Suppl. 2, 1, 1955.

(33) Johnson, H.L.: Lowell Obs. Bulletin, 4, 37, 1958.

(34) Johnson, H.L.: Astrophys. Journ. 126, 121, 1957.

(35) Johnson, H.L.: Astrophys. Journ. 126, 134, 1957.

(36) Johnson, H.L.: Ann D'Astrophysique 18, 292, 1955.

(37) Johnson, H.L.: Astrophys. Journ. 120, 325, 1954.

(38) Johnson, H.L.: Astrophys. Journ. 117, 357, 1953.

(39) Johnson, H.L.: Astrophys. Journ. 116, 272, 1952a.

(40) Johnson, H.L.: Astrophys. Journ. 116, 640, 1952b.

REFERENCES (Contd)

(41) Johnson, H.L. & Sandage, A.R.: Astrophys. Journ. 121 616, 1955.

(42) Johnson, H.L., Sandage, A.R. & Wahlquist, H.D.: Astrophys. Journ. 124, 81, 1956.

(43) Johnson, H.L. & Iriarte, B.: Lowell Obs. Bulletin 4, 47, 1958.

(44) Johnson, H.L. & Knuckles, C.F.: Astrophys. Journ. 122, 209, 1955.

(45) Johnson, H.L. & Hiltner, W.A.: Astrophys. Journ. 123, 267, 1956.

(46) Johnson, H.L. & Morgan, W.W.: Astrophys. Journ. 122, 429, 1955.

(47) Johnson, H.L. & Morgan, W.W.: Astrophys. Journ. 117, 313, 1953.

(48) Johnson, H.L. & Morgan, W.W.: Astrophys. Journ. 114, 522, 1951.

(49) Kushwaha, R.S.: Astrophys. Journ. 125, 242, 1957.

(50) Levee, R.D.: 117, 200, 1953.

(51) Lindholm, E.H.: Astrophys. Journ. 126, 588, 1957.

(52) Luyten, W.J.: Publ. Astronom. Obs. Univ. of Minnesota, 2, No. 7, 1939.

(53) Lynga, G.: Kungl. Svenska Vetenskapsakademien, Band 2, Nr. 34, Almqvist & Wiksell/Stockholm, 1959.

(54) Mestel, L.: Monthly Notices Roy. Astronom. Soc. 113, 716, 1953. (Also Astrophys. Journ. 126, 550, 1957).

(55) Milne, E.A.: Monthly Notices Roy. Astronom. Soc. 83, 118, 1923.

(56) Mitchell, R.I. & Johnson, H.L.: Astrophys. Journ. 125, 414, 1957.

(57) Naur, P. & Osterbrock, D.E.: Astrophys. Journ. 117, 306, 1953.

(58) Osterbrock, D.E.: Astrophys. Journ. 118, 529, 1953.

(59) Parenago, P.P.: Trudy Astronom. Inst. Sternberg 25, 1954.

REFERENCES (Contd.)

(60) Reiz, A.: Astrophys. Journ. 120, 342, 1954.

(61) Rhijn, P.J. Van: Groningen Publ. No. 47, 1936.

(62) Roberts, M.: Lecture Notes, International Summer Courses in Science, NUFIC, IV.8, The Hague, 1960.

(63) Salpeter, E.E.: Symposium on Astrophysics, (Ann. Arbor: University of Michigan), 1953.

(64) Sandage, A.R.: Stellar populations, Vatican Observatory, p. 287, 1958a.

(65) Sandage, A.R.: Stellar populations, Vatican Observatory, p. 149, 1958b.

(66) Sandage, A.R.: Stellar populations, Vatican Observatory, p. 41, 1958c.

(67) Sandage, A.R.: Stellar populations, Vatican Observatory, p. 75, 1958d.

(68) Sandage, A.R.: Astrophys. Journ. 125, 435, 1957a.

(69) Sandage, A.R.: Astrophys. Journ. 126, 326, 1957b.

(70) Sandage, A.R.: Astronom. Journ. 58, 61, 1953.

(71) Sandage, A.R.: Astrophys. Journ. 131, 598, 1960.
& Wallerstein, G.

(72) Sandage, A.R. & Schwarzschild, M.: Astrophys. Journ. 116 463, 1952.

(73) Sandage, A.R. & Van den Bergh: Lecture Notes, International Summer Courses in Science, NUFIC, IV.4, The Hague, 1960.

(74) Schönberg, M. & Chandrasekhar, S.: Astrophys. Journ. 96 161, 1942.

(75) Schwarzschild, M.: Structure and Evolution of Stars, Chap. VI, p. 208, Princeton Univ. Press, 1958.

(76) Schwarzschild, M.: Astrophys. Journ. 107, 1, 1948.

(77) Siedentopf, H.: A.N. 254, 33, 1934.

(78) Stebbins, J. & Whitford, A.E.: Astrophys. Journ. 102, 318, 1945.

REFERENCES (Contd.)

(79) Stebbins, J. & Whitford, A.E.: Astrophys. Journ. 87, 237, 1938.

(80) Stoy, R.H.: Vistas in Astronomy, Vol. 2, p. 1097, Pergamon Press, 1956.

(81) Strömgren, B.: Astronom. Journ. 57, 65, 1952.

(82) Sweet, P.A.: Monthly Notices 110, 548, 1950.

(83) Taylor, R.J.: Astrophys. Journ. 120, 332, 1954.

(84) Thomas, L.H.: Monthly Notices, Roy. Astronom. Soc., 91, 122, 619, 1931.

(85) Underhill, A.B.: Astrophys. Journ. 131, 124, 1960.

(86) Unsöld, A.: Physik der Sternatmosphären, 1938 (2nd Ed.), Springer, 1955.

(87) Van Beuren, H.G.: Bull. Astronom. Inst., Netherlands, 11, No. 432, 1952.

(88) Varsavsky, C.M.: Astrophys. Journ. 132, 354, 1960.

(89) Walker, M.F.: Astrophys. Journ. 125, 636, 1957.

(90) Walker, M.F.: Astrophys. Journ. Suppl. No. 23, 1956.

(91) Whitford, A.E.: Astronom. Journ. 63, 201, 1958.

(92) Wesselink, A.J.: Trans. I.A.U. 7, 269, 270, 1950.

(93) Ziepel, H.V.: Monthly Notices Roy. Astronom. Soc. 84, 665, 702, 1924.